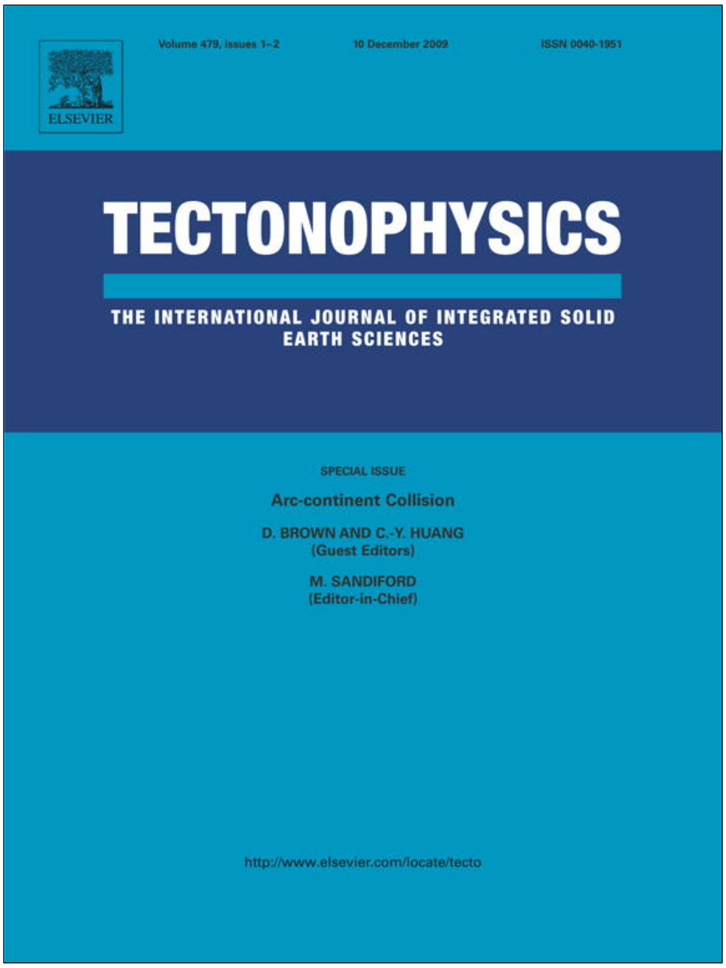
Volume 479, issues 1–2
10 December 2009
ISSN 0040-1951
ELSEVIER
TECTONOPHYSICS
THE INTERNATIONAL JOURNAL OF INTEGRATED SOLID EARTH SCIENCES
SPECIAL ISSUE
Arc-continent Collision
D. BROWN AND C.-Y. HUANG
(Guest Editors)
M. SANDIFORD
(Editor-in-Chief)
http://www.elsevier.com/locate/tecto

Tectonophysics 479 (2009) 66–94

Contents lists available at ScienceDirect

Tectonophysics

journal homepage: www.elsevier.com/locate/tecto

Tectonic evolution of forearc nappes of the active Banda arc-continent collision: Origin, age, metamorphic history and structure of the Lolotoi Complex, East Timor

Carl E. Standley, Ron Harris *

Department of Geological Sciences, Brigham Young University, Provo, Utah 84602-4606, USA

ARTICLE INFO

Article history:
Received 2 July 2008
Received in revised form 13 January 2009
Accepted 29 January 2009
Available online 14 February 2009

Keywords:
East Timor
Metamorphism
Arc-continent collision
Banda Arc
Structure
U/Pb age
Lu-Hf age
Accretion
Lolotoi Complex

ABSTRACT

An integrated multidisciplinary investigation of the Lolotoi Complex of East Timor (Timor Leste) indicates that it is part of the Banda forearc that was metamorphosed and rapidly exhumed during the Eocene and accreted to the NW Australian continental margin during Late Miocene to present arc–continent collision. Greenschist, graphitic phyllite, quartz–mica schist, amphibolite and pelitic schist dominate metamorphic rock types. Mineral, whole rock, and trace element geochemical analyses of metabasites indicate protolith compositions consistent with tholeiitic basalt and basaltic andesite with mixed MORB and oceanic arc affinities. Metapelite schist is mostly composed of metasedimentary units derived from mafic to intermediate rocks with oceanic to continental volcanic arc provenance.

Thermobarometric calculations show peak metamorphic conditions of 530 °C to 680 °C for garnet–biotite pairs and amphibole, and peak pressures of 5 to 10 kbar for garnet–aluminosilicate–quartz–plagioclase assemblages. Peak metamorphism occurred at 45.36 ± 0.63 Ma, as indicated by Lu–Hf analyses of garnet. Detrital zircon grains have a U/Pb age distribution with spikes at 663, 120 and 87 Ma, which is typical of detrital zircon ages throughout the Great Indonesian Arc of Asia, but is distinct from Australian affinity units. These data indicate deposition and later metamorphism occurred after 87 Ma.

Structural analyses of the metamorphic rocks and their sedimentary and volcanic cover units reveals 5–6 deformational phases of alternating shortening and extension. There is little to no evidence of strike-slip deformation. Phases 1–4 are inferred as pre-Oligocene from age determinations. Phases 5 and 6 are most likely related to latest Miocene to Pliocene nappe emplacement and Pliocene to present collisional deformation. Kinematic indicators show mostly top to the SE directed shortening and top to the south and SE extension. Structural mapping indicates that the Lolotoi Complex and some of its cover units are in thrust contact with underlying Gondwana Sequence rocks. Asian affinity volcanic and sedimentary cover units are found mostly in normal fault contact with metamorphic rocks.

These data indicate that the Lolotoi Complex of Timor Leste is correlative with the Mutis Complex of West Timor and both form part of the Banda Terrane, which is composed mostly of dispersed fragments of the eastern Great Indonesian Arc. The study demonstrates the complex nature and deformational history of forearc basement.

1. Introduction

The accretion of volcanic arcs to continents is a fundamental process of continental growth (e.g. Bailey, 1940; Taylor and McClennan, 1985; Jahn et al., 1998). Most commonly it involves the partial subduction of a passive continental margin, which results in accretion of large fragments of the upper plate, or even the complete arc–forearc system itself, to the continental margin. These processes can be investigated directly in the active arc–continent collision of the NW Australian continental margin with the Banda Arc of the SE Asian plate (Fig. 1). However, most studies of arc-related units in this region are only reconnaissance in nature due to inaccessibility and political unrest. For example, lack of reliable age constraints on metamorphic rocks in the Timor region have led to speculation that their origin ranges from Pre-Cambrian Australian basement (Grady, 1975; Chamalaun and Grady, 1978; Charlton, 2002) to Miocene collision-related complexes (Hamilton, 1979; Kaneko et al., 2007). Each of these interpretations requires vastly different arc-continent collisional models to explain. To better understand how best to use the Banda arc-continent collision as an analog for the numerous ancient arc-collisions that are responsible for most of Earth's continental crust, we have conducted an integrated multidisciplinary investigation of the Lolotoi Complex in Timor Leste. This unit exposes poly-deformed metamorphic rocks with sedimentary and volcanic cover units (Audley-Charles, 1968). Its origin and tectonic affinity is related to similar units in West Timor that are interpreted as slabs of the Banda forearc, but no data is available to test this correlation.

* Corresponding author.
E-mail address: rharris@byu.edu (R. Harris).

0040-1951/$ – see front matter © 2009 Elsevier B.V. All rights reserved.
doi:10.1016/j.tecto.2009.01.034

This study follows-up on an earlier, more regional investigation of the Banda Terrane published by Harris (2006). This paper provides age constraints ($^{40}Ar/^{39}Ar$, U/Pb and Rb/Sr) for metamorphic rocks at the highest structural levels in mostly West Timor, which indicate Oligocene igneous and metamorphic cooling and exhumation. Harris (2006) relates these events to the collisional demise and extensional collapse of the eastern Great Indonesian Arc, which was the eastern extension of the Sunda Arc. These events pre-date the Late Miocene to present arc-continent collision between the Banda Arc and the NW Australian passive continental margin.

The Banda arc-continent collision is used as a modern analog for many diverse types of collisional settings throughout time, including settings for the origin and emplacement of Oman-type ophiolites (e.g. Searle and Stevens, 1984; Harris, 1992).

However, recent investigations (Harris and Long, 2000), including this paper, reveal that most forearc thrust sheets on Timor are not ophiolites, and require a different model for their origin, although emplacement mechanisms may be similar to those of ophiolites (Harris, 1992). Questions about the origin and tectonic evolution of forearc regions that we address here are relevant not only to understanding the tectonic history of the Banda Orogen, but arc-continent collisional processes in general.

The regional significance of this study is that it tests for similarities and differences between the Lolotoi Complex of Timor Leste and other parts of the Banda Terrane throughout the Timor region. The Banda Terrane consists of fault-bounded rock bodies with compositions and ages that correlate with *in situ* units found in Sumba and the Banda Sea region (Audley-Charles and Harris, 1990). These rocks are currently part of the SE Asian Plate and mostly consist of fragments of the eastern Great Indonesian Arc. However, some parts of the Banda Terrane may have been derived from pieces of Australia and other parts of Gondwana (Milsom et al., 2001) that accreted to the Great Indonesian Arc before its extensional collapse in the Paleogene (Harris, 2006). In this paper we investigate this question by conducting a variety of age determinations, including U/Pb age analysis of detrital zircon grains in order to constrain whether units are derived from Australian or Asia.

2. Previous studies

Early studies of metamorphic rocks of the Banda Terrane in West Timor, which is known as the Mutis Complex, were conducted on a series of high-standing metamorphic and igneous massifs (Fig. 1B and C) that include: Lalan Asu (de Waard, 1954a,b, 1957), Mutis (de Roever, 1940; Sopaheluwaken, 1990; Harris, 1991, 1992; Harris and Long, 2000), Miomoffo (van West, 1941; Sopaheluwaken, 1989), Boi (Earle 1981; Brown and Earle, 1983), Mollo (Tappenbeck, 1939; Earle, 1980), Usu (de Waard, 1959), and Ocussi (Harris, 1992; Harris and Long, 2000). Most of these studies conclude that the metamorphic rocks and their cover successions are of Asian affinity and are thrust onto Australian continental margin units in an ‘Alpine-style’ of deformation, although emplacement age interpretations vary.

The Lolotoi Complex has received little attention. Although reconnaissance studies demonstrate that it is similar in composition and structural setting to Banda Terrane massifs in West Timor and other places (Audley-Charles, 1968; Harris, 1991, 1992), they are interpreted in widely differing ways (i.e. Charlton, 2002; Kaneko et al., 2007). This paper aims to provide the necessary petrologic, geochemical,

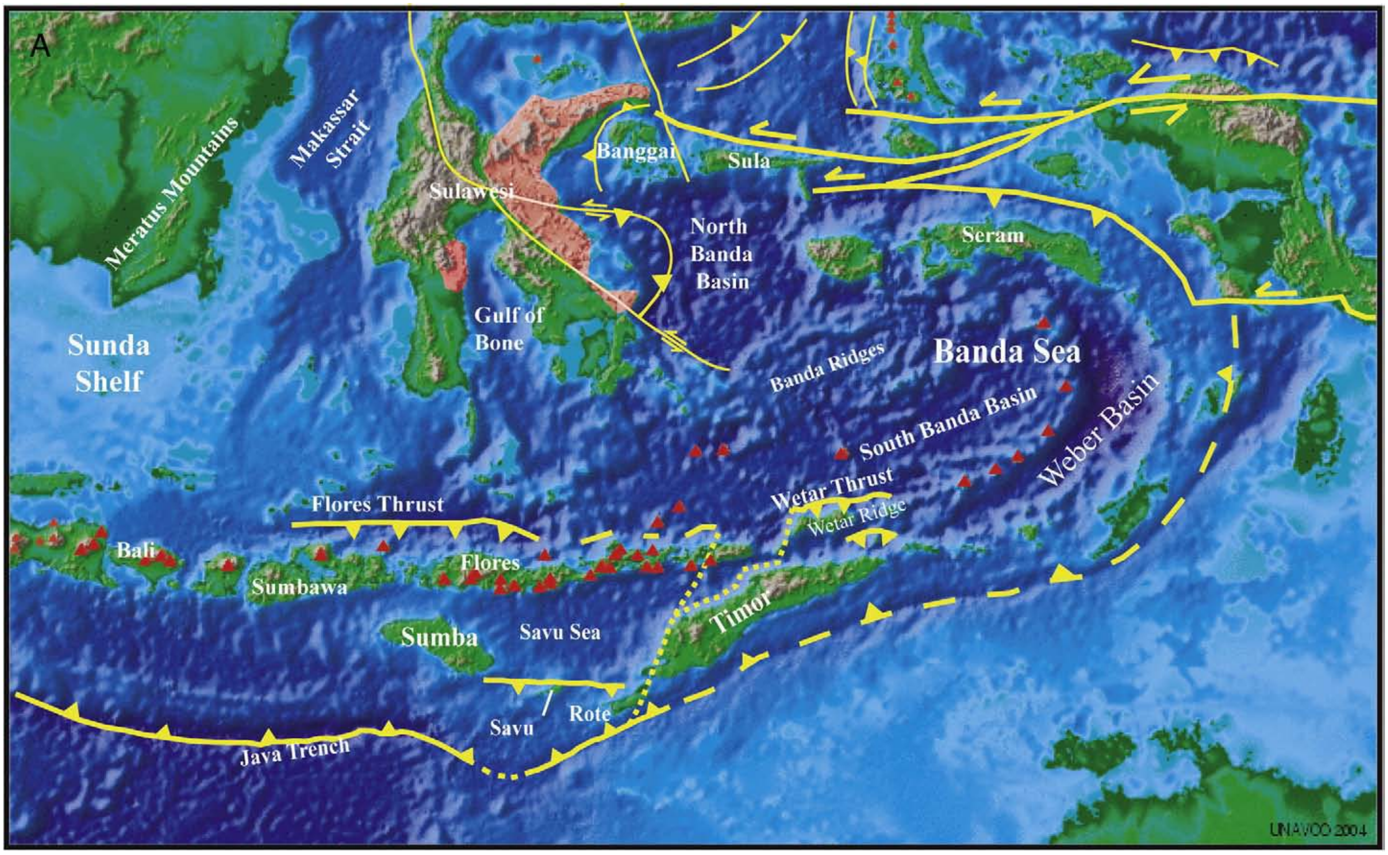

Fig. 1. A) Digital elevation model of the Banda Arc region. Active faults are shown in yellow, red triangles are active volcanoes, pink areas are regions of mafic and ultramafic rocks. The Makassar Strait, Gulf of Bone and Banda Sea occupy a region that was formerly the Cretaceous to Paleogene Great Indonesian Arc. Arc fragments, known as the Banda Terrane (Harris, 2006) are found in Sulawesi, the Banda Ridges, Sumba, Savu, Rote, Timor, and the volcanic islands around Flores and Wetar. B) Generalized geologic map of Timor taken mostly from Audley-Charles (1968) and Harris et al. (2000) showing various Banda Terrane massifs interpreted as structurally overlying Australian affinity Gondwana Sequence units. C) Cross section modified from Harris (1991) showing Timor as a young accretionary fold and thrust belt formed by underthrusting of Australian continental margin units beneath the Banda forearc.

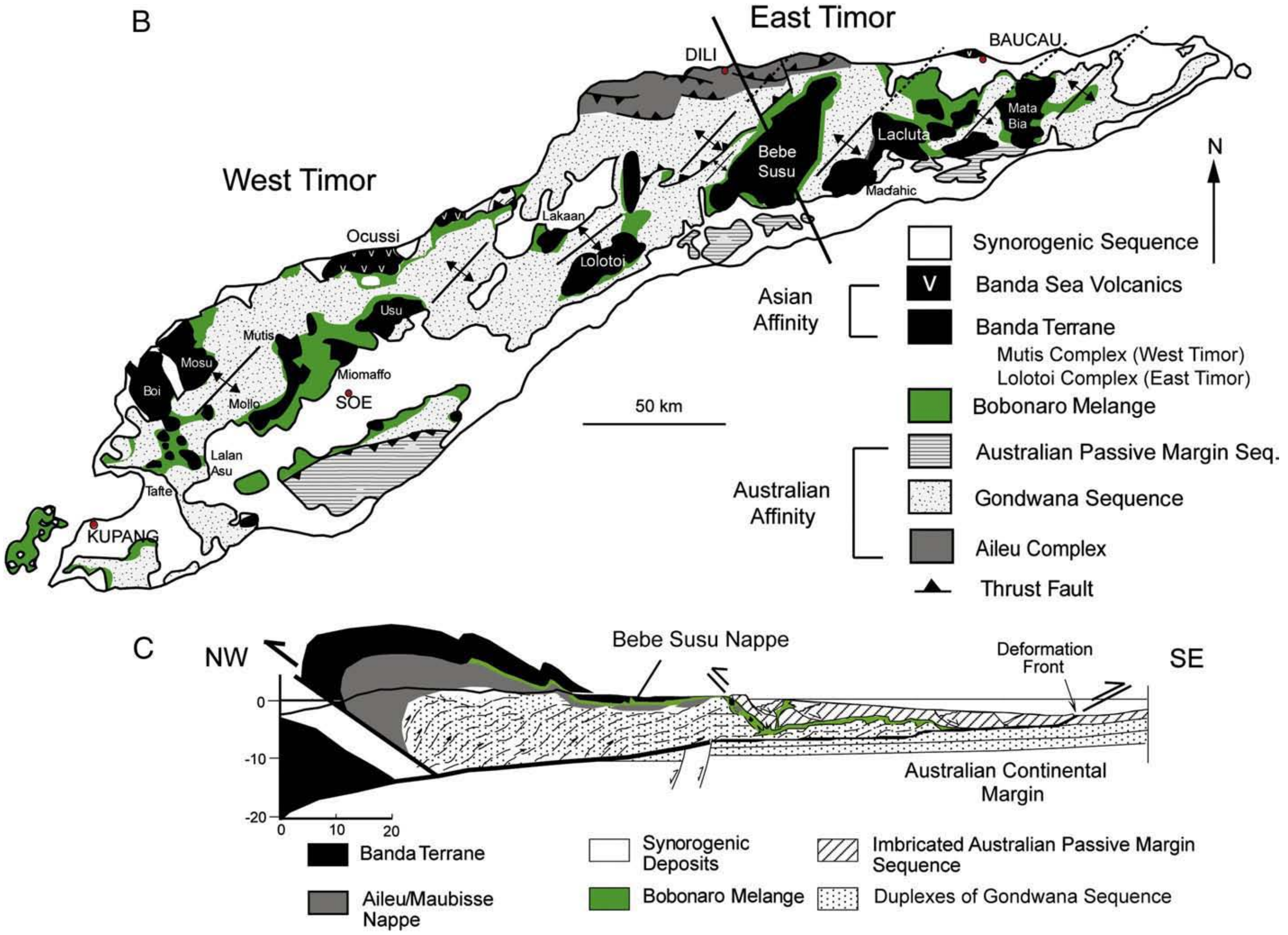

Fig. 1 (*continued*).

age, stratigraphic and structural constraints to distinguish between rival interpretations about the composition, origin, metamorphic history, and tectonic evolution of the Lolotoi Complex of Timor Leste. It also provides insights into the complex origin and age relations associated with accretion and exhumation of forearc basement.

3. Geological setting

Banda Terrane units in the Timor region are part of a series of high-level thrust sheets represented by up to 2000 km^2 isolated remnants of medium- to low-grade metamorphic rocks structurally overlain by Cretaceous to Miocene age volcanic and sedimentary cover units intruded by dikes (Fig. 2). Structural and stratigraphic relations not only establish the Banda Terrane as the uppermost structural unit in Timor, but also reveal stark differences in age and rock type between the Banda Terrane and units from the Australian continental margin. For example, the occurrence of Tertiary turbiditic units, carbonate with Asian affinity faunal assemblages, arc affinity volcanic rocks, and dikes have no equivalents in the passive continental margin of Australia, which was far from any plate boundary until its Late Miocene to present collision with the Banda Arc (Harris, 2006).

The Banda arc-continent collision began as the distal most reaches of the Australian continental margin accreted beneath and in front of the Banda forearc. Some of these units are exposed along the north coast of Timor and consist of lherzolitic peridotite and Permian to Jurassic Gondwana Sequence units. These units are associated with the Aileu Complex, which were metamorphosed by the Late Miocene to Pliocene initiation of collision. Continued convergence accreted progressively thicker and more proximal continental margin units. The clogging of the subduction channel by these units is manifest by rapid rates of Pliocene and Quaternary uplift along the southern edge of the Banda forearc (Cox et al., 2006; Roosmawati and Harris, 2009-this issue; Harris et al., 2009). Exposures of Banda forearc crust (Banda Terrane) are found in several places throughout the active arc-continent collision (Fig. 1). Some parts of the Banda Terrane are detached from their structural roots and emplaced over thrust stacks of Australian continental margin units to form high-level nappes.

High shear strains along the base of these thrust nappes are well documented by massive amounts of tectonic mélange (Fig. 1), which surrounds each of the nappes and is locally well exposed beneath them (Harris et al., 1998). These highly chaotic block-in-clay units are known as the Bobonaro Mélange, which grades downward into broken formation of fold and thrust sedimentary and igneous cover sequences of the Australian passive continental margin.

Australian continental margin cover consists of two different mega-sequences. The Gondwana Mega-Sequence consists of Permian–Jurassic units deposited in intra-cratonic regions of Gondwana before late Jurassic breakup. Gondwana breakup formed the NW Australian passive continental margin. Sedimentary and igneous units deposited on the passive continental margin unconformably overlie the Gondwana Sequence, and are known as the Australian Passive Margin Sequence (Haig et al., 2007). It consists of mostly of Cretaceous–Pliocene pelagic continental rise and slope deposits.

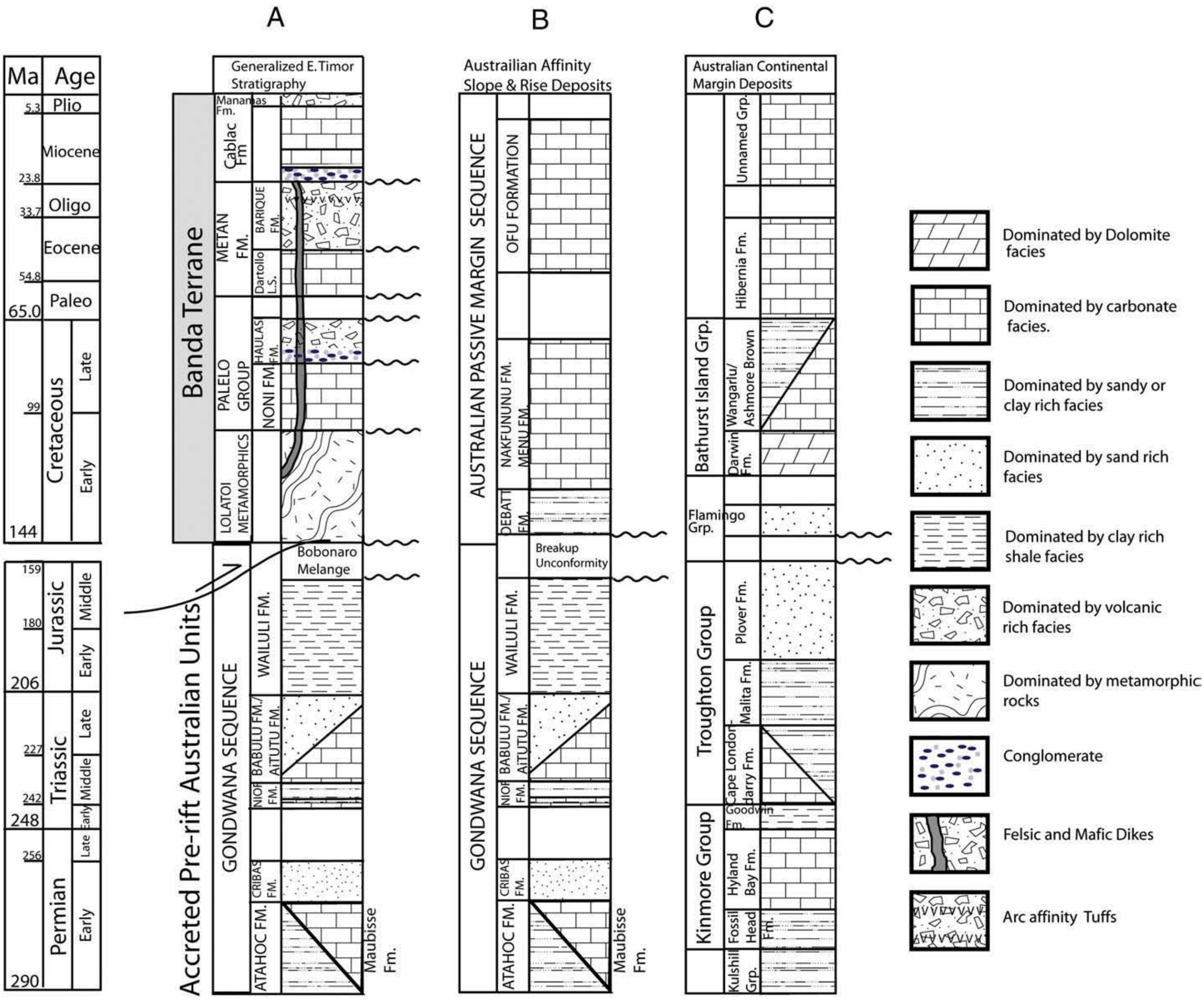

Fig. 2. Stratigraphic columns of A) lithotectonic units in Timor Leste, B) Australian slope and rise deposits accreted to the Banda Terrane, and C) Australian continental margin deposits. The Banda Terrane in Timor was thrust over Gondwana Sequence cover units of the Australian continent during Late Miocene to Pliocene arc-continent collision. Most of the Australian Continental Margin Sequence (formerly Kolbano Sequence) is accreted to the front of the Banda Terrane.

The uppermost unit of the Gondwana Sequence is the Wai Luli Formation, which consists of up to 1 km of smectite-rich mudstone (Audley-Charles, 1968). This unit acts as the uppermost major decollement for accretion of Australian Passive Margin Sequences to the southern edge of the Banda forearc to form the islands of Timor (Fig. 1C). The Wai Luli Formation also forms most of the matrix of mélange over which the Banda Terrane was tectonically emplaced (Harris et al., 1998). Continued underthrusting and duplex stacking of the Gondwana Sequence has uplifted Banda Terrane units to heights of 2500 m. Subsequent erosion removed much of the nonresistant Cretaceous to Tertiary sedimentary and volcanic cover units of the Banda Terrane roof thrust leaving mostly isolated remnants of metamorphic klippe (massifs). The most deeply exhumed parts of the collision are found in Central Timor with less exhumed sections to the west and east (Harris, 1991).

The largest area of Banda Terrane metamorphic rocks exposed in Timor is what we call here the Bebe Susu massif, after Bebe Susu Village near the middle of the nappe (Fig. 3). It has also been referred to as the Laclubar massif, after the town of Laclubar on its eastern edge. We prefer 'Bebe Susu' so that the massif is not confused with the Lacluta massif immediately to the east. The Lolotoi massif, after which the Lolotoi metamorphic complex gets its name, is immediately to the west of the Bebe Susu massif (Fig. 3). Like most part of the Banda Terrane, these massifs are preserved in synforms of the Timor fold and thrust belt. Traverses up streams in both the Lolotoi and Bebe Susu massifs provide access to many excellent outcrops of the interior of these mostly metamorphic bodies. Access to outcrops of the Lacluta massif is very limited, which restricted analyses to samples of float and stream boulders.

4. Composition

Metamorphic rock types found in the Lolotoi Complex of the three massifs we studied (Table 1) consist of medium pressure-temperature greenschist to amphibolite facies metasedimentary and meta-igneous units and are dominated by greenschist>graphitic phyllite>quartz–mica schist>amphibolite gneiss and schist>garnet bearing pelitic gneiss and schist (Figs. 4 and 5). We investigated the protolith and metamorphic history of these rocks using both mineral and whole rock geochemical analyses (Appendix A). A Cameca SX-50 electron microprobe was used to analyze mineral chemistry. Whole rock geochemical analyses were conducted using a Siemens SRS 303 XRF in

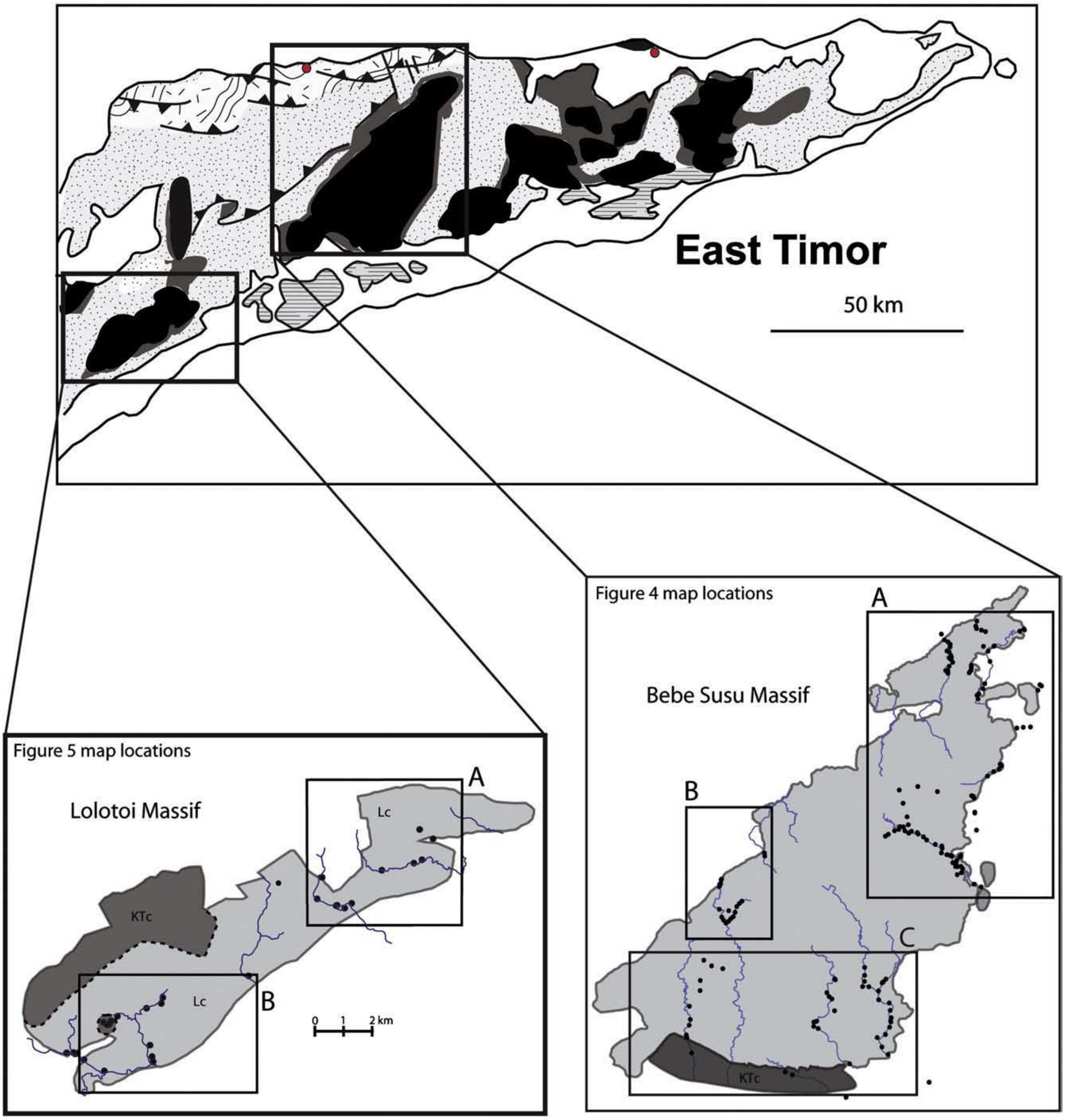

Fig. 3. Location maps of the Lolotoi and Bebe Susu Massifs. Black dots are sample locations and outcrops used for this study. Boxes are locations of maps in Figs. 4 and 5. The coordinates of all samples used in this study are provided in Table 1.

order to apply discriminant diagrams for determining protolith and tectonic affinity. For metamorphosed units only the most immobile elements (Ti, Zr, Y, Nb and Cr) are analyzed.

4.1. Greenschist units

Lolotoi Complex greenschist has a mineral assemblage of chlorite + quartz + plagioclase ± epidote ± muscovite ± minor apatite and sphene (Fig. 6B and Table 2). Samples are typically dominated by quartz or chlorite, with modal percentages of quartz ranging from 20 to 40% and amounts of chlorite from 40 to 50%. Chlorite grains are well-aligned and distinct chlorite-rich and quartz-rich domains on the mm to cm scale are common, though relatively homogenous non-layered textures are also common. Nearly complete retrograde alteration of plagioclase, muscovite, and biotite to fine-grained chlorite is characteristic. Quartz and especially carbonate veining is ubiquitous in most greenschist samples. Some layered carbonate-rich greenschist units consisting of quartz calc-schist and epidote–albite–calc schist are interpreted as originally impure limestone units. Similar units of greenschist are found throughout the Mutis Complex of West Timor (e.g. de Waard, 1957; Earle, 1981), and as blocks in mélange in Rote and Sawu (Harris, 2006) to the west of Timor (Fig. 1).

4.2. Amphibolite

Amphibolite in the Lolotoi Complex contains mostly green hornblende, blue amphibole (tschermakite and ferro-tschermakite) in one sample, + quartz ± plagioclase ± opaques ± muscovite,

Table 1

Massif	Sample #	Latitude (S)	Longitude (E)	Elev. (m)
Bebe Susu	7-16-2	8.61726	125.96311	182
	7-16-3	8.63379	125.93681	163
	7-16-4	8.62946	125.94158	1064
	7-16-5	8.6153	125.96664	1094
	7-17-2	8.75526	125.92406	1180
	7-17-4	8.75698	125.92473	1250
	7-19-2	8.76931	125.92543	174
	7-20-3	8.64906	125.92228	505
	7-22-4	8.67077	125.92721	354
	7-22-5	8.67073	125.92731	290
	7-27-1	8.60872	125.92725	474
	7-28-6	8.65007	125.90282	274
	7-30-4	8.81599	125.91529	616
	8-3-1	8.78577	125.87725	844
	8-3-2	8.78473	125.87228	748
	8-3-4	8.78433	125.86699	887
	8-3-5	8.7812	125.8656	842
	8-3-9	8.78718	125.85282	1274
	8-4-1	8.7792	125.86955	1402
	8-4-2	8.77258	125.86874	1366
	8-4-4	8.75013	125.86196	1376
	8-8-5	8.95482	125.85049	243
	8-8-7	8.96515	125.8476	237
	8-10-2	8.91151	125.84782	273
	8-10-5	8.897	125.85872	265
	8-11-3.5	8.91029	125.8328	360
	8-11-5	8.89858	125.83291	253
	8-13-1	8.98849	125.7726	246
	8-14-3	8.94795	125.79035	292
	8-15-2	8.92491	125.80565	393
	8-15-5	8.90867	125.80829	52
	F1-1	Float	Float	
	SF-2	Float	Float	
	SF-3	Float	Float	
	04T-70	8.94917	125.685032	400
Mata Bia	04T-10	8.581139	126.542111	576
	04T-16	8.642833	126.636028	688
	04T-9	8.598444	126.558444	1169
	04T-14	8.578417	126.678778	407
Lacluta	04T-ML0	Float	Float	
	04TML2	Float	Float	
	04T-34	8.866111	126.368694	22
	04T-MM-3	Float	Float	
	04T-MM-2	Float	Float	
	04T-MM-1	Float	Float	
	04T-MT-3	8.964582	125.652786	
Usu	MT-105F-91	9.531041	124.355194	
Mutis	MT-112-91	9.623779	123.684677	
Kisar (Aileu)	MT-44	8.021575	127.164735	32
	MT-45-1	8.023654	127.167056	66
	Mt-43	8.01975	127.160297	8

± biotite, ± chlorite ± epidote ± garnet. Apatite and sphene are abundant accessory minerals. Samples typically have modal percentages of hornblende ranging from 50 to 80% relative to quartz, and typically lack plagioclase (Table 2). The lack of plagioclase in most cases is due a protolith rich in silica, and in some cases to retrograde metamorphism to epidote–amphibolite facies. Hornblende grain size varies from very fine (<.05 mm) to coarse (>5 mm). Most samples are gneissic, having well-aligned amphibole grains with alternating amphibole-rich and quartz-rich bands. Schistose samples have relatively homogenous textures and tend to be more quartz-poor. Some samples have relict igneous textures with blebs of quartz and amphibole. Little, if any, micro-scale folding is present, though some brittle deformation is observed in gneissic samples.

4.3. Tectonic discrimination analysis

To better constrain the tectonomagmatic setting of amphibolite and greenschist units with relict igneous textures, and stratigraphically overlying non-metamorphosed volcanic rocks of the Barique Formation, we analyzed abundances of major, trace and rare-earth elements (Appendix A). Most of the samples we collected show chemical similarities to low-K tholeiitic basalt and basaltic-andesite with arc affinities (Fig. 7). Primitive mantle-normalized multi-element spider diagrams of these samples (Fig. 8) uniformly indicate subduction-related affinities based on low abundances of Nb and high LILE/HFSE ratios typical of back arc basin basalt.

To further test this result we applied a series of basalt discrimination diagrams to the relatively immobile elements (Ti, Zr, Y, Nb and Cr) in an attempt to minimize the effect of chemical homogenization during metamorphism or alteration. Most samples have characteristics of island arc basalt and MORB (Fig. 7). In some diagrams, Tertiary volcanic rocks of the Barique Formation overlap with meta-igneous units. These younger units are likely derived from a similar tectonomagmatic setting as the meta-igneous units they overlie.

Pearce (1996) gives examples of several marginal basin ridge systems above subduction zones that exhibit the type of hybrid compositions found in the Lolotoi meta-volcanic units and Barique Formation. These include the Valu Fa Ridge, East Scotia Sea; and Eastern Lau spreading centers. In terms of petrogenetic evolution, these chemical signatures most likely represent “melting at shallow levels of MORB mantle containing a variable subduction component, or by mixing of MORB-mantle and mantle wedge sources” (Pearce, 1996). Similar rock types are also found in dredge samples of the Wetar Strait north of Timor (Harris, 1992), Banda Sea Basin (Honthaas et al., 1998) and Sumba (Lytwyn et al., 2001).

Discrimination diagrams that we used for the provenance of metasedimentary pelitic rocks show mostly a source region that was mafic to intermediate in composition (Fig. 9). These results are consistent with interpretations that the Banda Terrane represents fragments of the Great Indonesian Arc, which collapsed by extension and rifted from the eastern margin of the Sunda Shelf during Eocene to Miocene supra-subduction zone seafloor spreading (Harris, 2006). Furthermore, the presence of abundant pelitic deep marine sedimentary units interbedded with volcanic units and abundant igneous intrusions without large plutons, indicates the original position of the Mutis and Lolotoi complexes was near, but off axis of a magmatic belt, likely in a proximal forearc basin position (Earle, 1981).

4.4. Pelitic units

The occurrence of pelitic units in the Lolotoi and Mutis Complexes has commonly been ignored in efforts to characterize the Banda Terrane as an ophiolite (see Harris and Long, 2000 for discussion). However, these units are one of the most important characteristics of the Banda Terrane because they provide constraints of metamorphic conditions and ages, and key provenance indicators. The most common pelitic unit is graphitic phyllite, which is composed exclusively of layers of graphite and quartz (Fig. 6A and C). The higher the abundance of graphite, the more fissile and less resistant the phyllite is, which controls to a large extent the limited vertical exposure in many parts of the Lolotoi complex.

Quartz–mica schist is less abundant, but is found throughout the Lolotoi Complex. It contains a main assemblage of quartz + muscovite ± biotite ± chlorite ± amphibole. Mica grains form well-defined foliations mostly parallel to quartz-rich and mica-rich compositional layering that resembles original depositional features of alternating of clay-rich and sand-rich layers (Fig. 10). Quartz domains dominate most samples, occupying from 40% up to 80% of the sample volume (Table 2). Muscovite is typically very fine-grained and deformed by folding with localized asymmetrical micro-folds indicating mostly top to the south vergence. Some samples exhibit well-defined S–C mylonitic fabrics (Fig. 10D).

Garnet-mica schist is relatively rare in the Bebe Susu and Lolotoi Nappes. It is characterized by biotite + muscovite + quartz + garnet +

plagioclase ± staurolite ± kyanite ± chlorite ± sillamanite. Garnet porphyroblasts are of two different types. Those in mostly mica-rich layers are idioblastic with rounded crystal faces. Those associated with quartz-rich layers are intensely resorbed forming xenoblastic grains. Most porphyroblasts are around 4 mm in diameter and show inclusions of quartz, epidote, ilmenite, biotite and plagioclase with only minor rotation during pre- and syn-kinematic growth (Fig. 11). Some alteration of garnet has occurred with mica at grain boundaries through net transfer reactions indicated by spessartine-rich garnet rims (Kohn and Spear, 2000). Kyanite porphyroblasts are up to 5 mm in length and are hybidioblastic to xenoblastic. Plagioclase compositions are principally andesine to labradorite (An20 to An67). Multiple generations of biotite growth are found as indicated by both syn- and post-kinematic relations (Fig. 11A). Retrograde alteration of mica, garnet and plagioclase to chlorite is common on grain boundaries, but for the most part this unit experienced little, if any retrograde metamorphism. Calcite veins are also rarely found.

Some samples from the southern Bebe Susu Nappe show inclusion free garnet preserved as cores inside inclusion-laden overgrowths. This texture most likely formed by changes in reaction during progradation of garnet growth rate. Microprobe X-ray dot maps confirm the occurrence of two growth intervals or phases of metamorphism (Fig. 12), which is also reported in some pelitic units in the Mutis Complex (Earle, 1981).

Earle (1981) describes retrogression and veining as the main metamorphic phenomena operating on Mutis Complex rocks after peak of metamorphism. This also is the case for the Lolotoi Complex, as retrogression of garnet, amphibole, and plagioclase to mica and

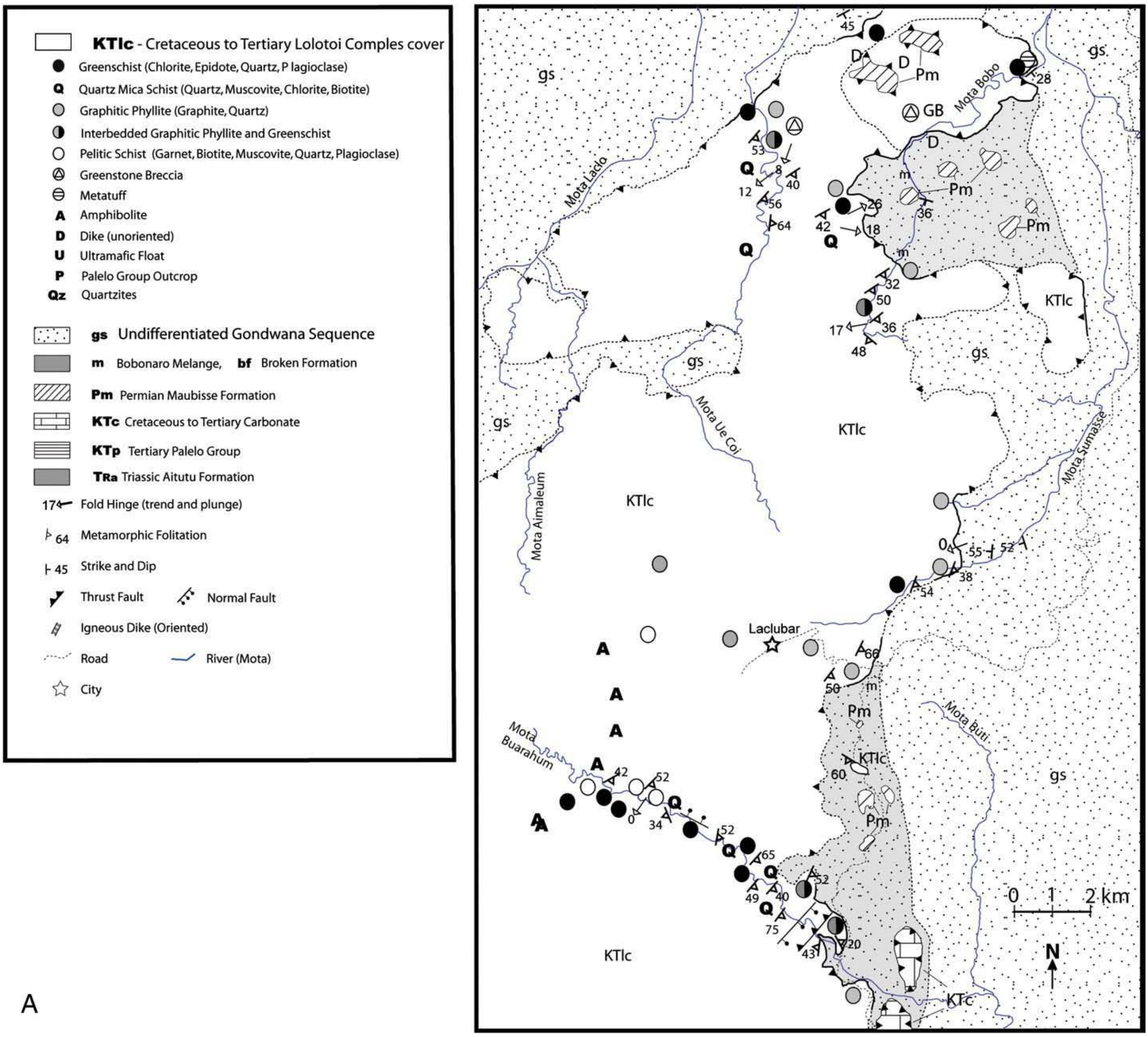

Fig. 4. Metamorphic units of the Lolotoi Complex in the Bebe Susu Massif. See Fig. 3 for location of maps. Most common metamorphic lithologies at each outcrop are shown. A) NE portion of the Bebe Susu massif. Note the presence of Permian Maubisse limestone only on the fringes and in erosional windows through the thin northern portion of the nappe, and the presence of mélange on the NE and SE portions of the map area. These contact relations document the flat-lying nature of the thrust contact between the Lolotoi Complex and underlying Australian affinity units (Harris et al., 1998). B) NW part of the Bebe Susu massif on the southern flank of the NE plunging Aitutu Anticline, which has warped the structural base of the massif. Most blocks in mélange are composed of fragments of the Aileu–Maubisse Nappe that structurally underlies the Bebe Susu Massif. C) SW part of the Bebe Susu nappe. Notice Asian affinity cover units found in normal fault contact with Lolotoi metamorphic units.

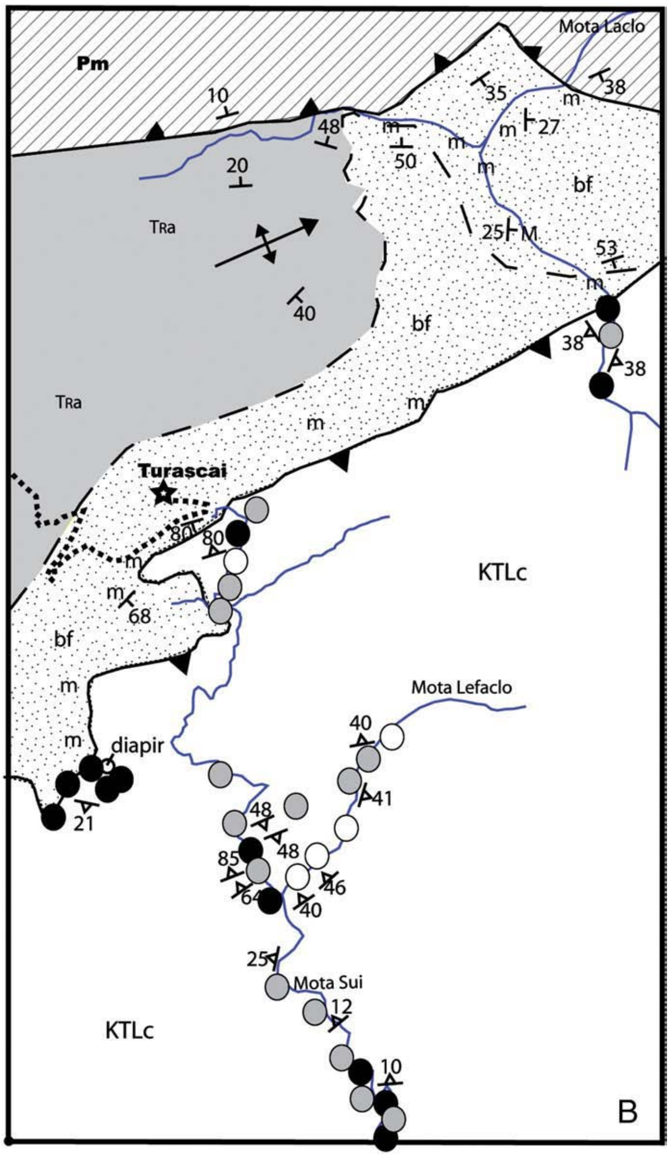

Fig. 4 (*continued*).

chlorite is widespread. Veining is extensive in greenschist, but rare in amphibolite or pelitic schist.

5. Field relations

Various lithologies in the Lolotoi Complex alternate at multiple scales, commonly several times at outcrop scale. The scale of these heterogeneities and lack of exposure outside of streambeds renders most individual units untraceable. Yet, compositional patterns are observed in the general distribution of dominant rock types in the Bebe Susu and Lolotoi massifs (Figs. 4 and 5). Graphitic phyllite is interbedded with all other metamorphic rock types present, but it is more abundant on the fringes of the nappes.

Alternating greenschist and quartz–mica schist dominate the majority of the interior of the nappes, though they are commonly inter-fingered with graphitic phyllite. Garnet-mica schist, and mica schist inter-finger with greenshist and graphitic phyllite in outcrops of isolated, deeply eroded areas of the central part of the Bebe Susu massif.

Investigations of the Mutis Complex in West Timor (de Waard, 1959; Earle, 1981) note a similar frequent alternation of rock types for much of the crystalline schist in the Usu, Lalan Asu, and Mutis massifs, which were interpreted as sedimentary in origin. Amphibolite is exposed in the central part of the Bebe Susu massif and is widespread in float. Locally, brecciated greenstone is found near the structural base of the Bebe Susu Nappe at both its northern and southern edges. Harzburgite, lherzolite, serpentinite, and altered gabbro are found locally as float. Mafic and felsic igneous dikes are found locally within each of the areas we investigated. Clasts in a boulder conglomerate found structurally overlying the southern edge of the Bebe Susu Nappe include abundant intermediate composition plutonic igneous material mixed with metamorphic clasts of the units described above.

Vertical successions of metamorphic units in the Lolotoi Complex are more difficult to determine than for thicker massifs with reportedly steep vertical metamorphic gradients, such as at the Mutis massif of West Timor (Sopaheluwaken et al., 1989).

However, it is apparent from field relations that lower grade greenstone, greenstone breccia and graphitic phyllite are found near the base of the nappes; greenschist and quartz mica schist are more abundant toward the interior; and the highest grade amphibolite and pelitic schist is found only in outcrop at the heart of the Bebe Susu Nappe. If the Bebe Susu massif is layered so that the interior represents a higher structural level, then it is similar to the general stacking relationship found in most massifs of the Mutis Complex (i.e. Earle, 1980; Sopaheluwaken, 1990). In both regions the metamorphism is generally inverted, which we interpret as a product of thrust stacking of deeper, higher-grade units above shallower, lower-grade ones. It is also possible that this relationship may be associated with channel flow. It is also important to note that structural field studies of the Mutis massif in West Timor (Harris and Long, 2000; Harris, 2006) and the Lolotoi Complex (see below) reveal that post-metamorphic low-angle normal faulting disrupts much of the metamorphic package, which complicates interpretations of metamorphic gradients and inversion.

Similarities between the Lolotoi and Mutis Complexes led Audley-Charles (1968) and others who have conducted field studies in both East and West Timor (Barber and Audley-Charles, 1976; Harris, 1991) to consider these metamorphic units parts of the same lithotectonic terrane. More peridotite is reported in some Mutis Complex massifs (Earle, 1981; Harris and Long, 2000), but the field relations of many of the peridotite bodies are poorly known. Peridotite bodies in the Mutis massif are both above and below metamorphic units (Harris and Long, 2000). It remains unclear which peridotite bodies are part of the Banda Terrane (associated with the pre-collisional accretionary wedge) or are exhumed parts of the most distal Australian passive margin (Harris and Long, 2000; Fallon et al., 2006), which would have been one of the first Australian affinity units accreted to the Banda Terrane.

6. Provenance

The question of provenance for the Lolotoi Complex is critical to reconstructing the tectonic evolution of the Banda Orogen. The Asian affinity of the Mutis Complex was initially inferred from field studies of its structural position (Wanner, 1913), overlying unmetamorphosed cover units (Tappenbeck, 1939), and metamorphic history (Brown and Earle, 1983). More recently these inferences were confirmed by $^{40}Ar/^{39}Ar$ age analyses of various mineral phases from multiple massifs of the Mutis Complex (Harris, 2006). However, none of these types of studies have been conducted on the Lolotoi Complex of Timor Leste.

Petrographic and petrologic studies indicate that most of the Lolotoi Complex was originally a succession of fine-grained clastic sediment interbedded with sandstone, limestone, tuffs and volcanic rocks. Whole-rock geochemical analyses (Appendix A) indicate that the volcanic rocks are subduction-related, and sedimentary units have an intermediate to mafic source region. These compositional characteristics are not found in age-equivalent units of the NW Australian

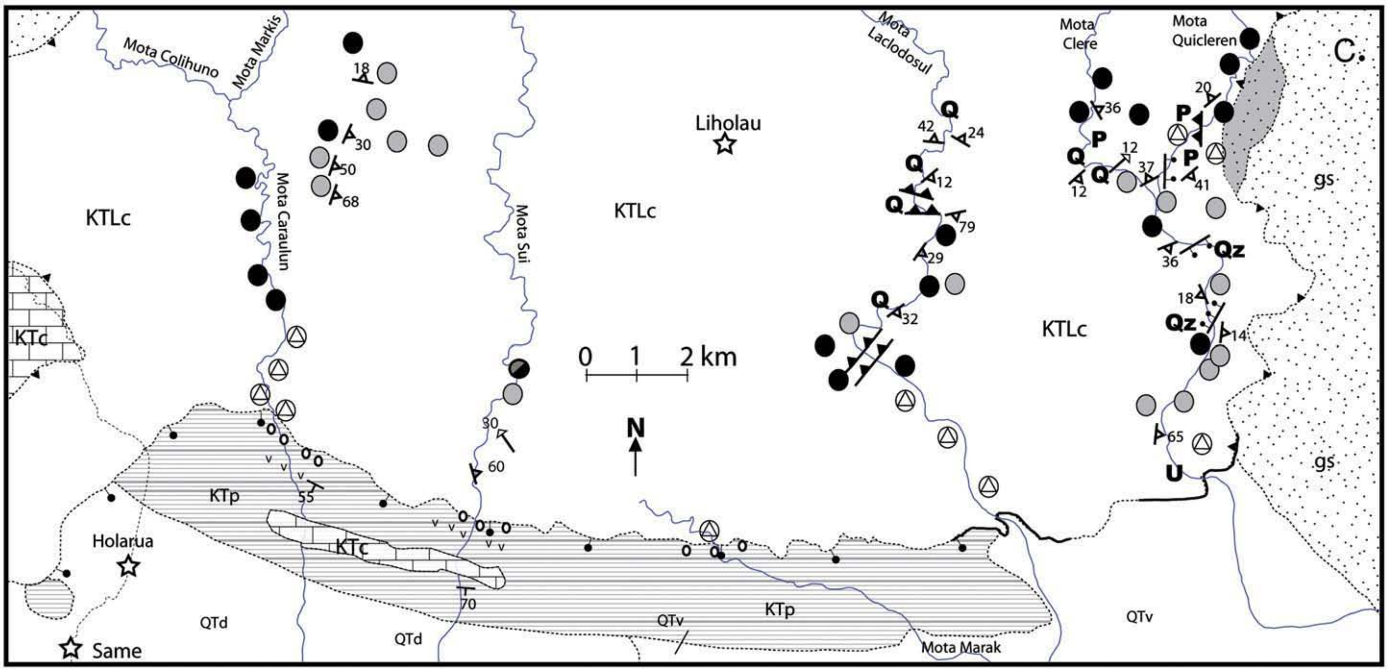

Fig. 4 (*continued*).

margin, but are very similar to *in situ* parts of the Banda Terrane, such as Sumba and southern Sulawesi.

7. Metamorphic conditions

We investigated the pressure-temperature conditions of the Lolotoi Complex by analyzing garnet, amphibole, plagioclase, biotite, and muscovite grains in garnet–mica schist, garnet–amphibolite and garnet-bearing greenschist from both outcrop and float samples collected in the Lacluta and central to southern portions of the Bebe Susu massifs (Appendix A). Eight different samples were studied to determine growth episodes, zoning profiles, retrograde effects, and geothermobarometric conditions.

Microprobe X-ray major element map images (Fig. 12) show most zoning profiles that are indicative of one single episode of garnet growth typical of normal growth zoning during prograde metamorphism (Banno et al., 1986). Mn and Ca decrease in abundance from core to rim while Mg and Fe increases. Zoning anomalies due to retrograde reactions are rare and mostly at grain boundaries and around large inclusions. Spessartine (Mn) spikes at rims in conjunction with irregular grain boundaries indicate some retrograde net transfer reactions have taken place (Kohn and Spear, 2000).

Biotite compositions are consistent across grains, except where retrograde alteration to chlorite has occurred, which is manifest by low K levels. K values below 9 wt.% are not used in geothermometry calculations. Biotite grains in contact with garnet and matrix grains were both analyzed. Compositions are close to those of the standards, which suggest that the analytical results should be reliable.

Plagioclase compositions vary significantly from sample to sample. All analyses lie along the Ca–Na solid solution, with compositions mostly of andesine and labradorite. No potassium feldspars are found.

Garnet grains were paired with neighboring biotite grains to obtain estimates of peak metamorphic temperatures. Care was taken during pairing of mineral analyses to use compositions characteristic of peak conditions. In samples with evidence of retrograde exchange reactions, peak conditions are represented by garnet with the highest Mg/Fe ratios and biotite with the highest Fe/Mg ratios (Kohn and Spear, 2000). These compositions correspond spatially in garnets rim areas, just inside of any alteration halos. Where retrograde reactions have occurred, the analyses represent minimum estimates of peak conditions, as possible higher conditions may have been lost to resorption.

The garnet–biotite thermometer of Kleemann and Reinhardt (1994) yields temperatures ranging from 530 °C to 600 °C. Garnet–aluminosilicate–quartz–plagioclase pairings yield pressures ranging from 6 to 8 kbars, using the Newton and Haselton (1981) barometer (Fig. 13).

Amphibole analyses include 10 samples from the Bebe Susu and Lacluta massifs (Fig. 14). Most amphibole compositions fall into the hornblende and magnesio-hornblende compositional fields, with the exception of one amphibole, which straddles the tschermakite and ferro-tschermakite fields (classified based on Leake, 1997). Amphibole analyses include rims, cores, and intermediate positions to determine the range of temperatures through which the grains grew (Fig. 14). Temperature and pressure estimates use single mineral amphibole geothermobarometry based on calculations by Gerya et al. (1997). Nine samples range from 6 to 7.5 kbar and 580 °C to 650 °C $\pm$ 1.2 kbar and 37 °C. One sample with ferrotchermakite yields a pressure of 9 to 10 Kbar and 650 °C to 680 °C. Traverses across amphibole grains show a consistent 2 kb decrease from core to rim, which indicates nucleation initiated near peak conditions and amphibole growth proceeded as pressure dropped.

7.1. Discussion

Pressure–temperature (*P–T*) estimates obtained from mineral geochemistry of Mutis massif rocks in West Timor were previously interpreted to show a steep inverse metamorphic gradient (Sopaheluwaken et al., 1989). Our results from the Lolotoi Complex do not support this interpretation. *P–T* data from garnet bearing pelitic rocks overlap with those from amphibolite samples, with slightly higher peak temperatures in amphibolite and slightly higher peak pressures in garnet-bearing pelite.

Similar geothermobarometric results are obtained in West Timor by Sopaheluwaken (1990), who reports garnet–biotite temperatures of 550 °C to 750 °C and GASP pressures of 6.0 to 8.6 kbars. Metabasic rocks were also evaluated by amphibole–plagioclase, and garnet–amphibole mineral pairs, and amphibole only that yield temperature

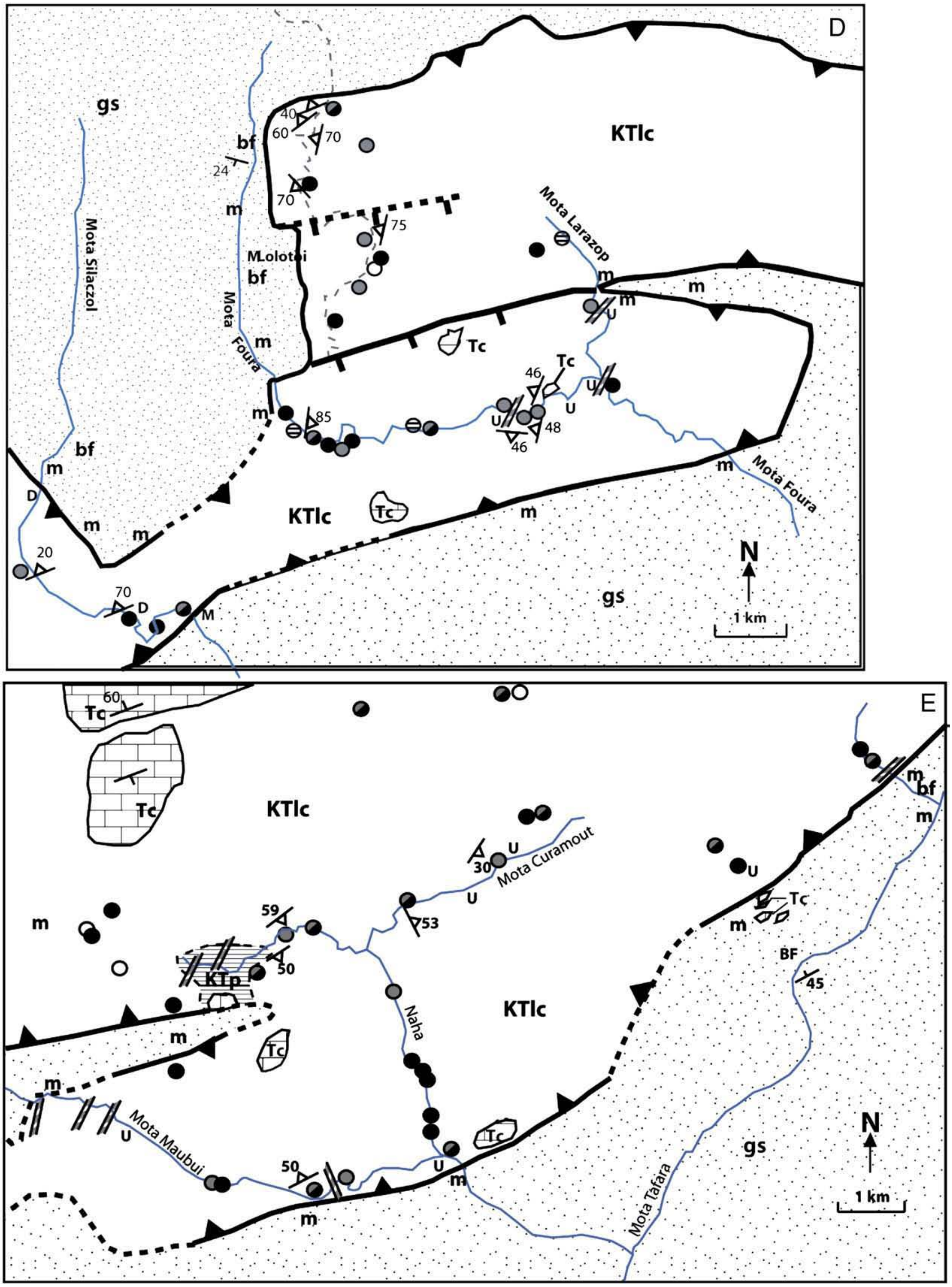

Fig. 5. Metamorphic units of the Lolotoi Complex in the Lolotoi Massif. See Fig. 3 for map locations and Fig. 4 for key to symbols. KTc are Cretaceous and Tertiary Asian affinity cover units.

of 510 °C to 580 °C and pressures of 6.2 to 8.2 kbars (Sopaheluwaken, 1990). This temperature range is significantly lower than that of the metapelites, even though pressures estimated for both rock types are nearly identical. Sopaheluwaken (1990) also analyzed a sample of granulite float at the highest structural levels of the Mutis massif, which yielded temperatures up to 950 °C and pressures up to 10.7 kbar. No similar granulite facies rocks are found in the parts of the Lolotoi Complex we could access. Besides the granulite sample,

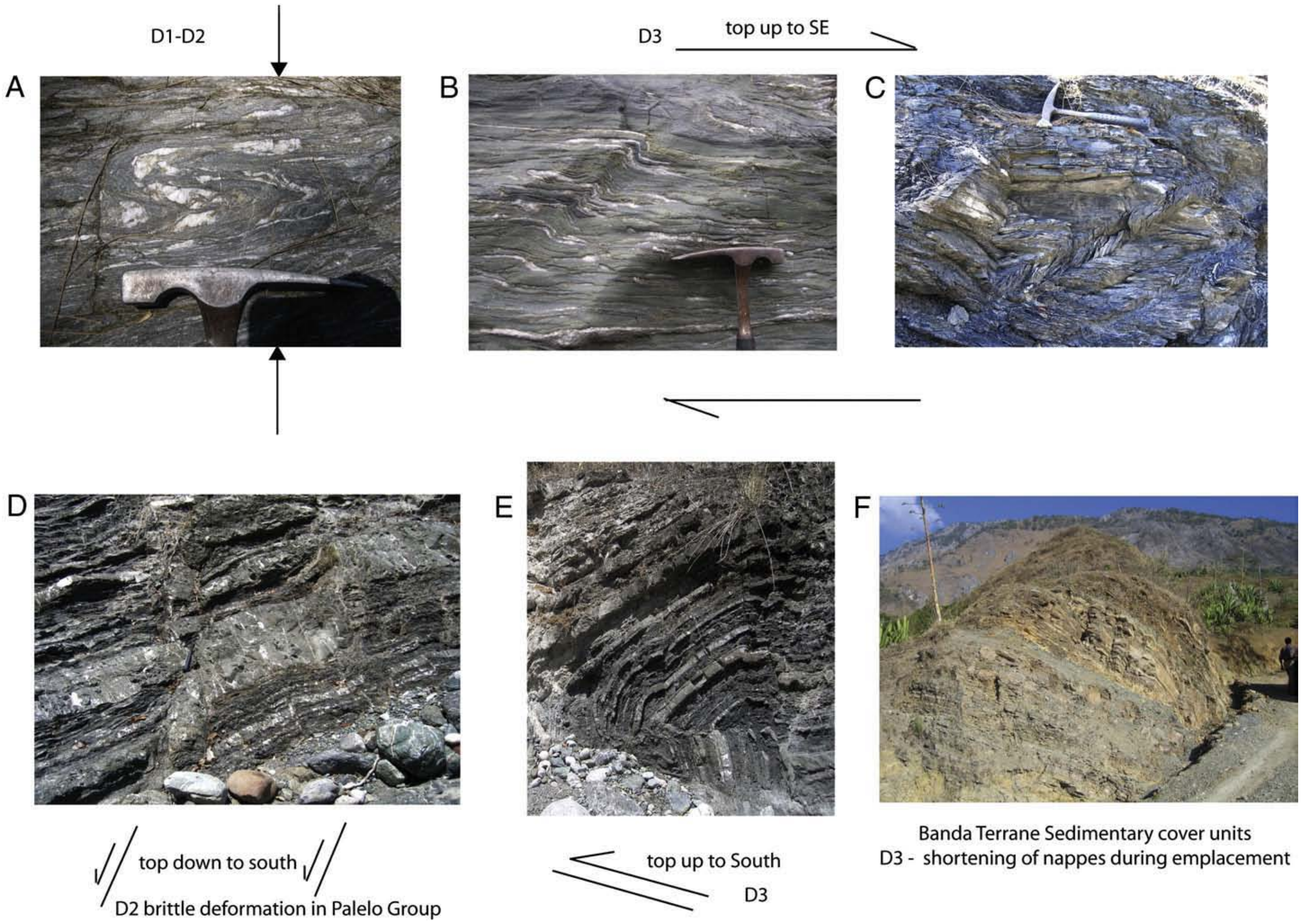

Fig. 6. Greenschist facies units of the Lolotoi Complex and its sedimentary cover. A) Graphitic schist with isoclinally folded composite S_0–S_1–S_2-parallel quartz veins. Looking to SW. B) Multiply deformed greenschist with isoclinal folded S_2 foliation refolded by top to SE D_3 (F_2). Looking to NNE. C) Graphitic schist with only one detectable folding event similar in orientation and fold asymmetry to F_3. S_3 crenulation cleavage is parallel to fold axial surfaces. Photo is looking NE. D) Folded pelagic turbidites of the Haulasi Formation (D_3). E) Top down to the SE normal faults offsetting folded Haulasi Formation units (D_2). F) Sedimentary and volcanic cover of the Lolotoi Complex of the Mata Bia Massif. Metan Formation (foreground) overlain by intermediate volcanic flows and tuffs, and unconformably overlying massive Cablac Limestone (background). Photo is looking south. See 'Structural Analysis' for explanation of textures.

there are no significant differences in metamorphic conditions between metapelitic and metabasic rocks of the Mutis and Lolotoi Complexes of West and East Timor, respectively. Both complexes have T/depth ratios of ~27 °C/km.

Brown and Earle (1983) note in their investigation of pelitic schist and amphibolite in the Boi and Mutis massifs an early high-pressure assemblage of garnet (preserved as homogenous core areas in now retrograded garnet porphyroclasts) + Al silicate + biotite + plagioclase +

Table 2
Modal abundance of metamorphic minerals.

Minerals	Metabasites							Metapelites						
	Amphibolites				Greesnschist			Garnet bearing schists				Quarts–mica schists		
	8-3-9	8-4-2	8-3-5	8-4-4	Bobo-2	04-WS_2	04T-ML6	8-3-5	F1-1	SF-3	04T-MILO	Clere	7-26-7	7-17-14
Quartz	15%	20%	40%	40%	20%	40%	30%	40%	50%	30%	40%	40%	80%	60%
Biotite									20%	20%	35%	10%	10%	
Muscovite									10%	8%	15%	20%	10%	35%
Chlorite			20%		50%	40%	40%	20%	5%			20%		
Plagioclase				5%					5%	10%	2%			
Garnet				5%					10%	30%	5%			
Epidote					5%	2%	10%							
Opaques	4%	2%	5%	5%	<1%	3%	<1%	5%	1%	<1%	3%	10%		5%
Hornblende	80%	75%	20%	50%				20%						
Calcite					20%	15%	20%							
Pyrite			10%					10%						
Staurolite									<1%					
Kyanite									5%	2%				
Zircon								%						
Apatite	<1%	1%	<1%	<1%				<1						
Sphene	<1%	1%	<1%	<1%				<1%						

quartz + opaques. They document a later lower pressure assemblage of cordierite + biotite + plagioclase + sillimanite + quartz ± hercynite ± opaques, with retrograde garnet and relict plagioclase. These assemblages in addition to geothermobarometric calculations are interpreted as evidence of early high *P–T* conditions (pressures ~10 kbar and temperatures >750 °C), which were followed by intermediate temperature (600–700 °C), low pressure (3–4 kbar) conditions associated with decompression. These estimates yield a *T*/depth ratio of 58 °C/km.

Most garnet-mica schist samples collected from outcrops in the Bebe Susu massif exhibit just a single generation of garnet growth. No textural or compositional characteristics of amphibolite indicate a polymetamorphic history, and their close proximity to outcrops of monometamorphic pelitic schist suggests an identical metamorphic history. Descriptions of monometamorphic assemblages in most other massifs of eastern West Timor are identical to those presented here for the Lolotoi Complex.

If differences in the metamorphic history of parts of the Mutis and Lolotoi complexes are within error, it could indicate local metamorphic gradients exist where a more extensive intermediate temperature late stage metamorphism produced low-pressure assemblages containing cordierite and sillimanite. This contrasts with the more common lower temperature retrograde event in other the eastern Mutis massifs and the Lolotoi Complex.

The discovery of intermediate temperatures and pressures, in conjunction with previously discussed igneous provenance, indicates that the Lolotoi Complex may have been metamorphosed by both magmatism and tectonic burial, and that the western Mutis Complex may have been closer to magmatic centers or regions of higher rates of lower crustal flow. Similar metamorphic rocks are found throughout the SE margin of the Sunda Shelf, Sumba and in fragments of the Great Indonesian Arc scattered throughout the Banda Sea (Harris, 2006). Most of these occurrences formed along the southeastern convergent margin of Asia prior to late Eocene to early Oligocene extensional collapse of the arc (Harris, 2006).

8. Age determinations

One of the most fundamental ways to test various tectonic affinity hypotheses and similarities for the Lolotoi and Mutis Complexes is to investigate ages of metamorphic mineral growth and cooling. Are these units 1) of Asian affinity with a Great Indonesian Arc association (Earle 1981), 2) a slab of Pre-Cambrian Australian metamorphic basement (Charlton, 2002), or 3) part of the Australian lower plate metamorphosed during Miocene to Pliocene collision (Kaneko et al., 2007).

Previous geochronological studies of the Mutis Complex show that it has a maximum protolith age of 200 Ma and a minimum

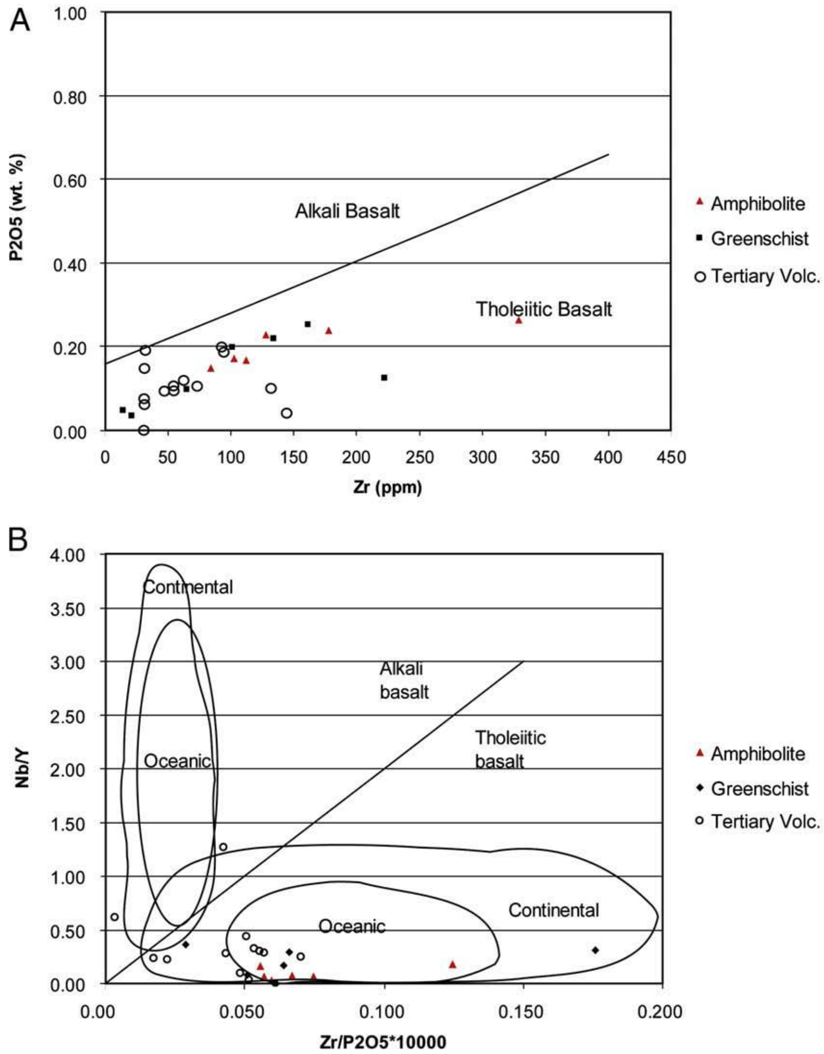

Fig. 7. Igneous discrimination diagrams comparing meta-volcanic rocks (amphibolite and greenschist with relict igneous textures) with Tertiary volcanic rocks of the Oligocene Barique Formation. A — Winchester and Floyd (1976), B — Floyd and Winchester (1975), C — Pearce (1982), D — Pearce and Cann (1973), E — Pearce and Gale (1977), F — Pearce (1982).

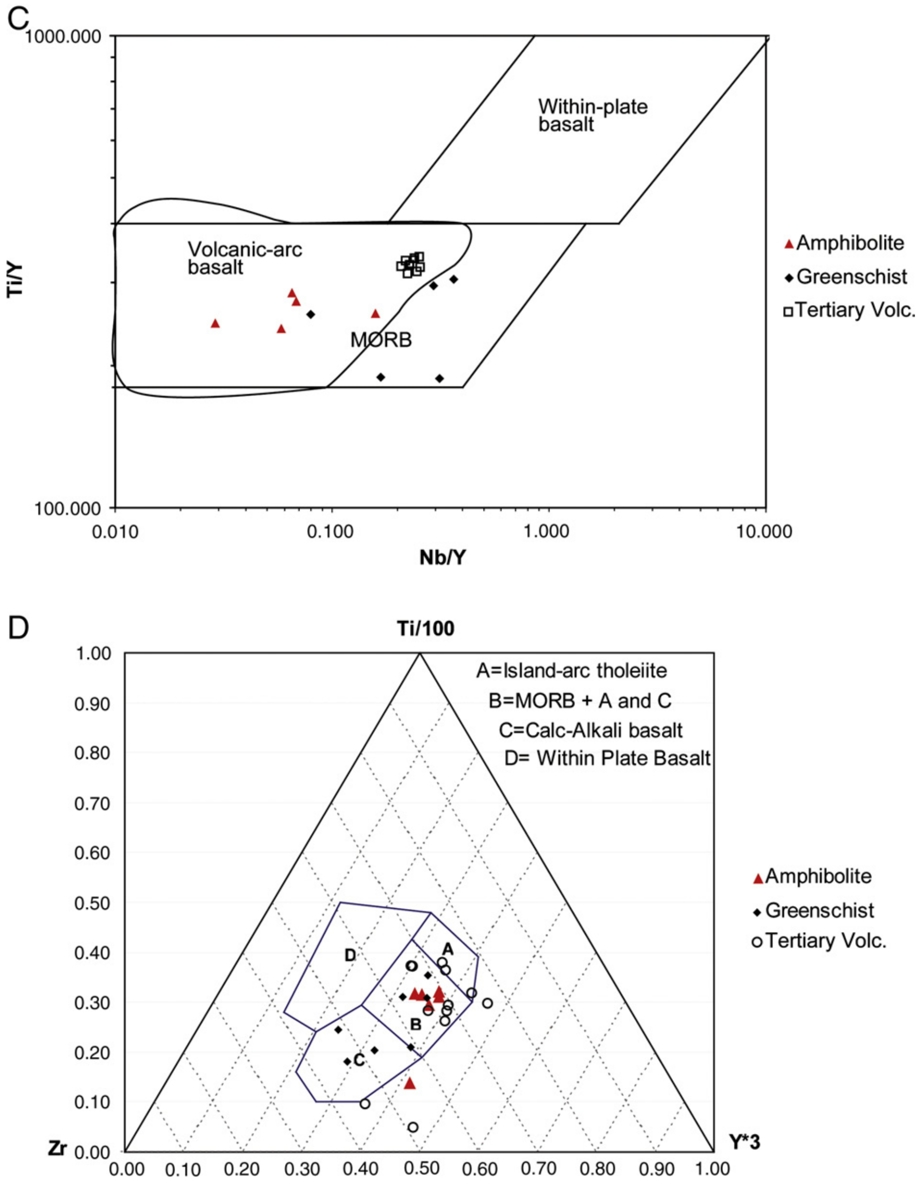

Fig. 7 (*continued*).

metamorphic age of 32 Ma based on whole-rock Rb/Sr analyses (Earle, 1981). Dacite overlying the Mosu massif of the western-most Mutis Complex has a U/Pb age of 35 Ma, and an andesite cobble in weakly metamorphosed conglomerates overlying Lolotoi Complex metamorphic rocks of the Bebe Susu Nappe has an age of 83 Ma (Harris, 2006). $^{40}Ar/^{39}Ar$ age analysis of hornblende and mica from five different massifs in the Mutis Complex yield plateau ages of metamorphic cooling ranging from 34–39 Ma (Harris, 2006). These results from the Mutis Complex and Palelo Group eliminate hypotheses 2 and 3. However, with no radiometric age determinations some have continued to argue that the Lolotoi Complex of Timor Leste may be different in origin and age than the Mutis Complex of West Timor. In this study we use multiple techniques to determine the age of detrital zircon (U/Pb), timing of garnet growth (Lu/Hf), and exhumation (apatite fission track) of Lolotoi Complex units.

8.1. U–Pb age analysis of detrital zircon grains

Only one sample (8-3-9) of the many we processed from each metamorphic unit of the Lolotoi Complex has detrital zircon grains. It is from the Bebe Susu Massif, and based on textural evidence and bulk geochemistry, this sample is most likely a meta-sediment. Zircon grains in the sample are of two different types: small, round extremely abraded and pitted grains, and more abundant subhedral lightly abraded grains with preserved crystal terminations (Fig. 15). U/Pb age analysis of these grains (Table 3) was performed using a Thermo-Finnigan Element2 Laser Ablation-ICP-MS at Washington State University.

Each of the different grain types produced widely different age distributions. The small, abraded grains yield ages mostly in the range 598–763 Ma and a mean age of 663 ± 12 Ma (Fig. 15). In contrast, euhedral grains show two peaks in the probability distribution: the highest occurs at 87.0 ± 2.7 Ma, and the smaller peak at 113.9 ± 8.3 Ma. The youngest grain is 81.8 ± 2.3 Ma, which is the maximum age of the sedimentary protolith.

The source of the latest Proterozoic and Cambrian zircon grains is likely the Pan African Pinjarra Orogenic Belt, which is also identified as the source of zircon grains found in basement rocks in SE Java. Smyth et al. (2007) report a major concentration of Cambrian to Late Proterozoic ages in Tertiary sandstone and volcanic rocks that may stretch from Java northeastward to Sulawesi. The source region was most likely rifted away from the western margin of Australia

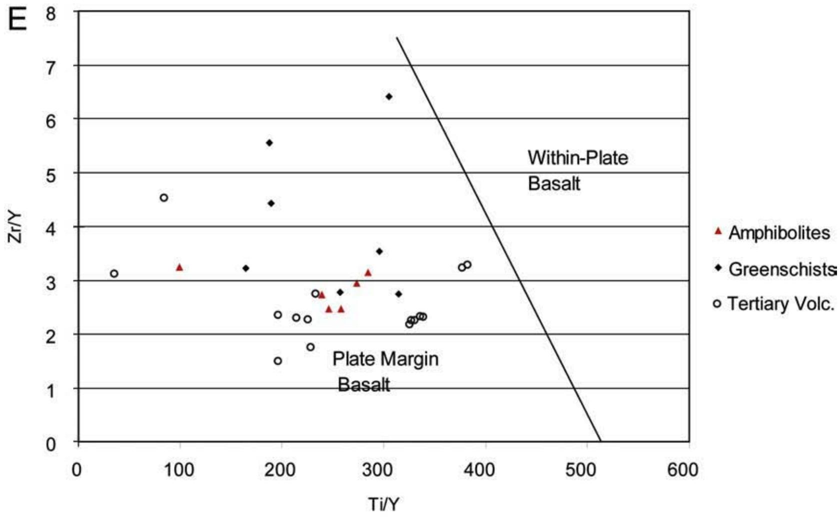

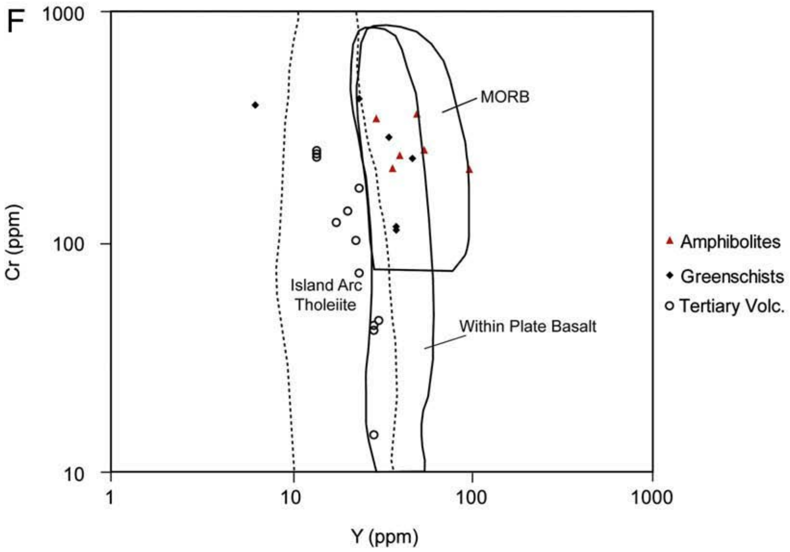

Fig. 7 (*continued*).

during Gondwana break up, and then accreted to the Great Indonesian Arc during the Late Cretaceous (Smyth et al., 2007).

The source for the euhedral grains is most likely the Great Indonesian Arc, which is mounted on stretched continental crust of the Sunda Shelf. The greater abundance and less abrasion of the younger grains indicates that they did not travel as far.

The Banda Terrane U/Pb age fingerprint is very different from that of Permian–Triassic units of Australian continental margin units that show two major concentrations of detrital zircon ages at 301 Ma and 1882 Ma, and some grains as old as 2456–2738 Ma (Harris, 2006; Zobell and Harris, 2007). The Australian affinity units are clearly of different origin than the Lolotoi metamorphic unit we sampled,

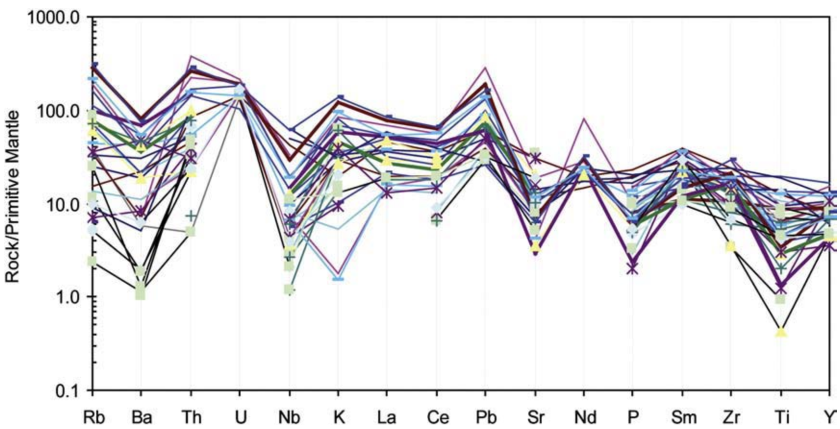

Fig. 8. Primitive mantle normalized multi-element spider diagram for samples from the Bebe Susu, Lacluta and Lolotoi Massifs. Normalization is based on McDonough and Sun (1995). Included in the plots are analyses from greenschist, amphibolite and relatively unaltered igneous rock. Notice the negative niobium anomalies present in most samples, indicating a subduction related origin.

which eliminates the possibility that the Lolotoi Complex is the metamorphic basement of the Australian Passive margin (Charlton, 2002), or its Permian–Jurassic sedimentary cover (Kaneko et al., 2007).

8.2. Lutetium–hafnium age determinations of garnet

To better constrain the age of metamorphism we conducted ^{176}Lu/^{176} Hf analysis (Table 4) of garnet grains with fewest inclusions in garnet-mica schist from the Bebe Susu and Lacluta massifs (Fig. 3). Samples were then analyzed using a ThermoFinnigan Neptune ICP-MS multi-collector at Washington State University. The lutetium–hafnium radiogenic isotopic system in garnet provides an age of its growth (Blichert-Toft and Frei, 2001), which is essentially the maximum age of metamorphism.

Four samples of similar composition were analyzed: 04 T-MLO (Al_{65-75}, Gr_{10-15}, Py_{6-10}, Sp_{5-10}), SF-2 (Al_{60-70}, Gr_{10-13}, Py_{6-13}, Sp_{15-20}), 8-3-5 (Al_{60-67}, Gr_{12-14}, Py_{7-10}, Sp_{10-20}), and 8-3-2 (Al_{60-70}, Gr_{10-20}, Py_{3-13}, Sp_{3-13}). Sample preparation followed the methods of Patchett and Ruiz (1987), Vervoort and Patchett (1996) and Vervoort et al. (2004). Separation of Hf and Lu from each other and other constituents was performed using multiple stages of column chemistry similar to those outlined by several authors (Patchett and Tatsumoto, 1980; Vervoort and Patchett, 1996; Vervoort and Blitchert-Toft, 1999).

Isochrons for the four samples give ages of 46.5 ± 1.2, 45.2 ± 0.4, 45.4 ± 3.3, and 46.4 ± 0.7 (errors are 2 s) with a weighted mean age of 45.4 ± 0.7 Ma (Fig. 16). The validity of an isochron depends upon its MSWD (mean squares of weighted deviates) value, which should be <2.5 (Rollinson, 1993). Two of the isochrons have MSWD values below this number, and the other two produce ages within the error limits of the acceptable isochrons (Fig. 16).

Since the garnet grains we analyzed have textural evidence of only one generation of growth, it is unlikely that any subsequent event heated them above the closure temperature of the Lu–Hf system. Therefore, we interpret this age to represent a portion of the prograde path near peak metamorphism. Unfortunately, only garnet

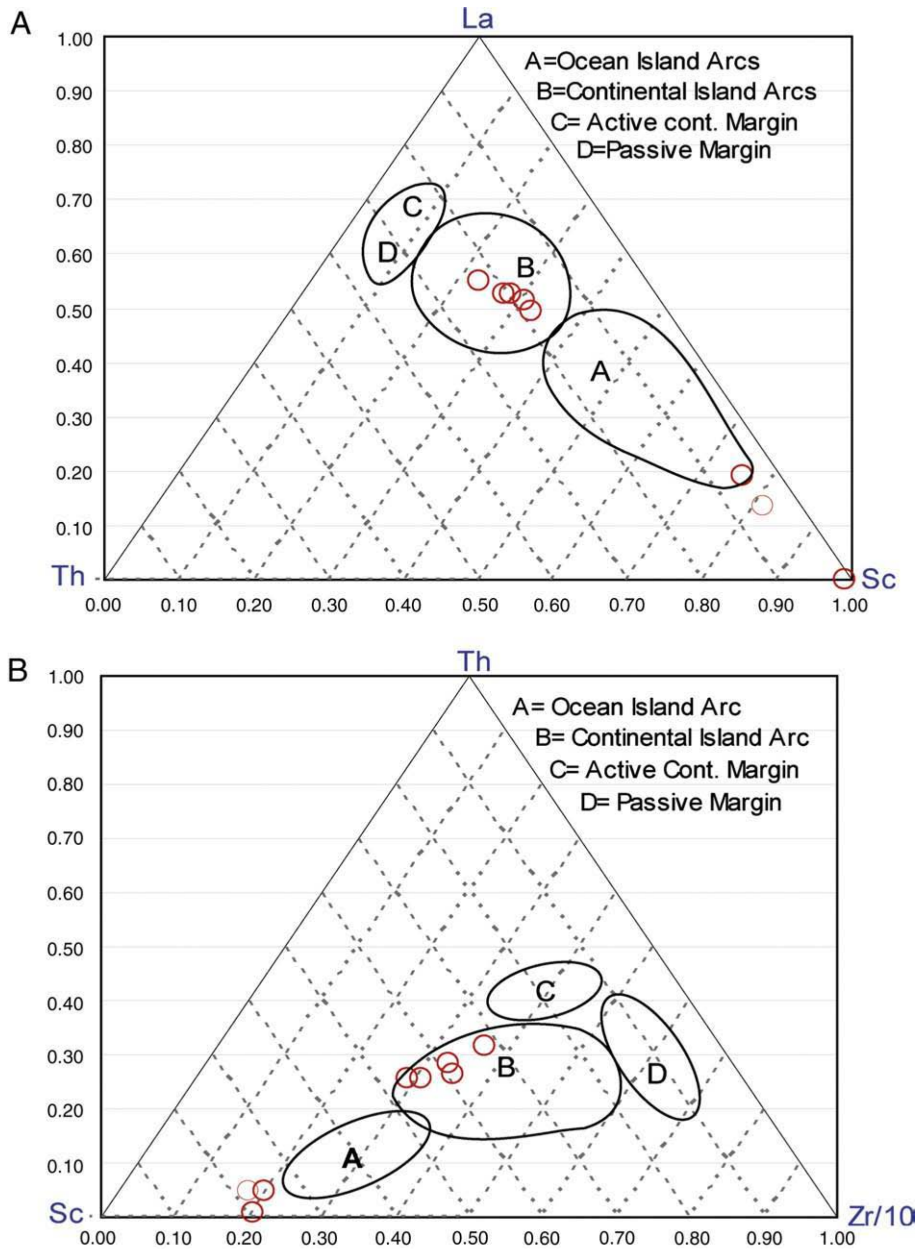

Fig. 9. Discrimination diagrams for metapelites showing associations with continental and oceanic arcs, and mafic and intermediate igneous provenance. A and B — Bhatia and Crook (1986), C — Bhatia (1983), D — Roser and Korsch (1988).

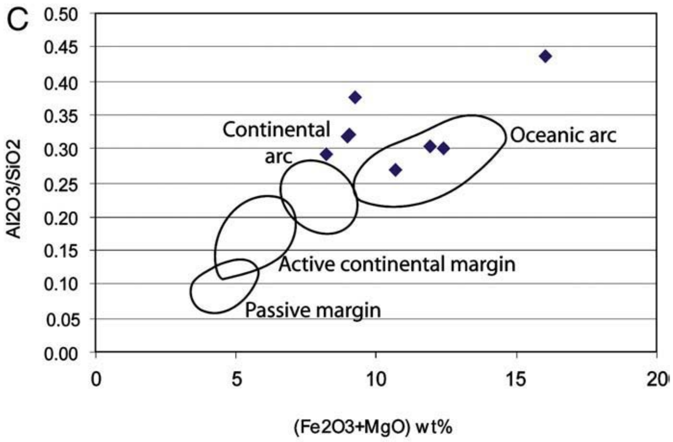

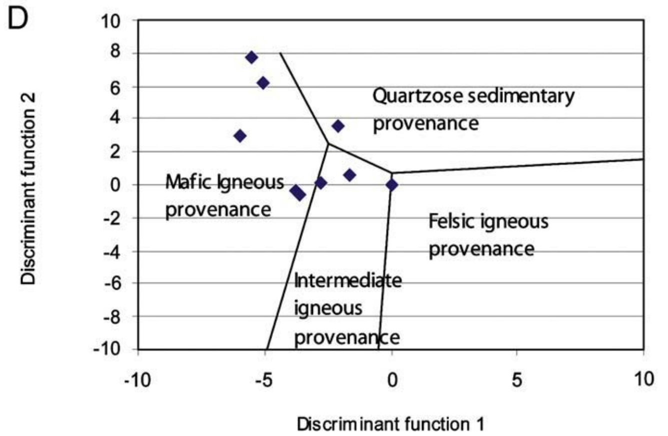

Fig. 9 (*continued*).

without inclusion trails can be analyzed, which eliminates the possibility of age determinations on obvious syn- or post-kinematic garnet. Sample 04 T-MLO is enclosed by foliation (Fig. 11A), which is indicative of pre-kinematic growth. The other three samples show equivocal evidence of either pre- or synkinematic growth. Since the ages are concordant, the textural relations reveal that most deformation occurred after 45 Ma.

While Lu–Hf analyses of Mutis Complex garnets have not previously been performed, K/Ar and $^{40}Ar/^{39}Ar$ analyses of various mineral phases from five different massifs in West Timor (Mosu, Boi, Mollo, Mutis , and Usu) are reported. K–Ar ages published by Earle (1980) and Sopaheluwaken (1990) range from 31 to 38 Ma. $^{40}Ar/^{39}Ar$ ages for hornblende separates range between 34.0 ± .03 to 38.6 ± 2.2 Ma (Harris, 2006). The difference of 7 Ma between metamorphism at around 650 °C and cooling to 500 °C, which is the closure temperature of the $^{40}Ar/^{39}Ar$ system in hornblende (Mezger, 1990) could be from relatively slow cooling or may represent different metamorphism events.

8.3. Apatite fission–track age determination

The cooling history of metamorphism can be further constrained by apatite fission track analysis. Metamorphic cooling ages for the Mutis Complex using $^{40}Ar/^{39}Ar$ age determinations of amphibole (34–39 Ma), muscovite (34–37 Ma) and biotite (33–34 Ma) produce a cooling curve showing the metamorphic rocks moved from depths of around 18 km to the surface in 6 my. (Harris, 2006). Assuming a thermal gradient of 27 °C/km based on thermobarometric estimates, these data yield a rock uplift rate of 3 mm/year, which is consistent with the development of a major unconformity between the Lolotoi Complex and overlying conglomerates and limestone of Oligocene–Miocene age.

Apatite fission-track age determinations (Table 5) were performed to investigate if the Banda Terrane was subsequently disturbed by any other low temperature events associated with its Pliocene obduction onto the NW margin of Australia during the Banda Orogen. Twelve samples from Banda Terrane massifs in Timor Leste, West Timor, and Aileu Complex units in Kisar were examined. Mounted apatite grains were polished, exposed to Californium-252 radiation and chemically etched to expose horizontal tracks just below the surface. Only two samples contained sufficient track density to produce viable horizontal track length information. Histograms of horizontal track length measurements show no long 16 to 18 µm tracks, indicating uplift from the partial annealing zone must have taken place in the last few million years (Fig. 17).

Due to the low density of fission tracks and the abundance of defects in the grains, ages were determined using the fission-track population method described by Naeser (1976, 1979), and more recently by Naeser et al. (1989) and Donelick et al. (2005). In the population method track counts from many grains are pooled to obtain a single age for the entire sample, rather than an age for each individual grain as in the external detector method (Fleischer et al., 1964; Naeser and Dodge, 1969). Eight samples were rejected due to: 1) scarcity of fossil tracks from low uranium values, 2) lack of apatite grains, and 3) inconveniently high numbers of induced tracks that made accurate determination of track densities unreliable.

One age of 41 ± 13 Ma was obtained for a sample from the Mutis Massif, and three ages of 20 ± 2 Ma, 18 ± 2 Ma and 12 ± 1 Ma were obtained from Aileu Complex metamorphic rocks collected on the island of Kisar, just east of Timor. No track length distribution data is available for the Kisar samples. However, other units from the Gondwana Sequence yield similar ages with track-length distributions demonstrating apatite grains were partially reset and in the partial annealing zone before rapid exhumation, which was so recent that no new tracks were found.

The Mutis Massif sample has a relatively high error due to low numbers of both fossil and induced tracks. In addition, frequent blemishes and irregularities in the apatite grains reduce the accuracy of track counts and most likely produce an inflated age. An inflated age is also consistent with $^{40}Ar/^{39}Ar$ cooling ages of 39–34 Ma reported from various mineral phases of the Mutis Complex (Harris, 2006). The minerals dated have closure temperatures much higher than that of the partial annealing zone and indicate the 41 Ma fission track age is suspect, and is most likely younger.

Another way to calculate the age is through modeling its thermal history. Model ages (Fig. 18) were constructed from track length measurements, calculated ages, etch pit diameters and user defined time-temperature constraints using AFTsolve 0.8.3 software designed by Ketcham et al. (2003). Major time-temperature constraints used in inverse modeling include: 1) 45.6 Ma age of peak metamorphism, which corresponds to temperatures of approximately 600 °C; 2) temperatures near 20 °C at 28 Ma, which is the age of the unconformity between metamorphic rocks and unmetamorphosed conglomerate and carbonate units (Harris, 2006); and 3) current exposure at the surface at 20 °C. Using these constrains yielded a statistical best-fit model age of 23 Ma. Fission-track length distributions predicted by the model closely match those observed (Models A and C, Fig. 18). Model B uses only beginning and end constraints, and is included as a measure of uniqueness of solutions A and C.

All of the models we ran require rapid rock uplift from forearc basement depths of around 4–5 km to a high-level thrust sheet elevation of around 1 km during the past 2–3 my. These estimates predict long-term rock uplift rates that range from 1.5 to 2 mm/year. These rates are within the range of direct measurements of long-term surface and rock uplift rates based on analysis of foraminifera

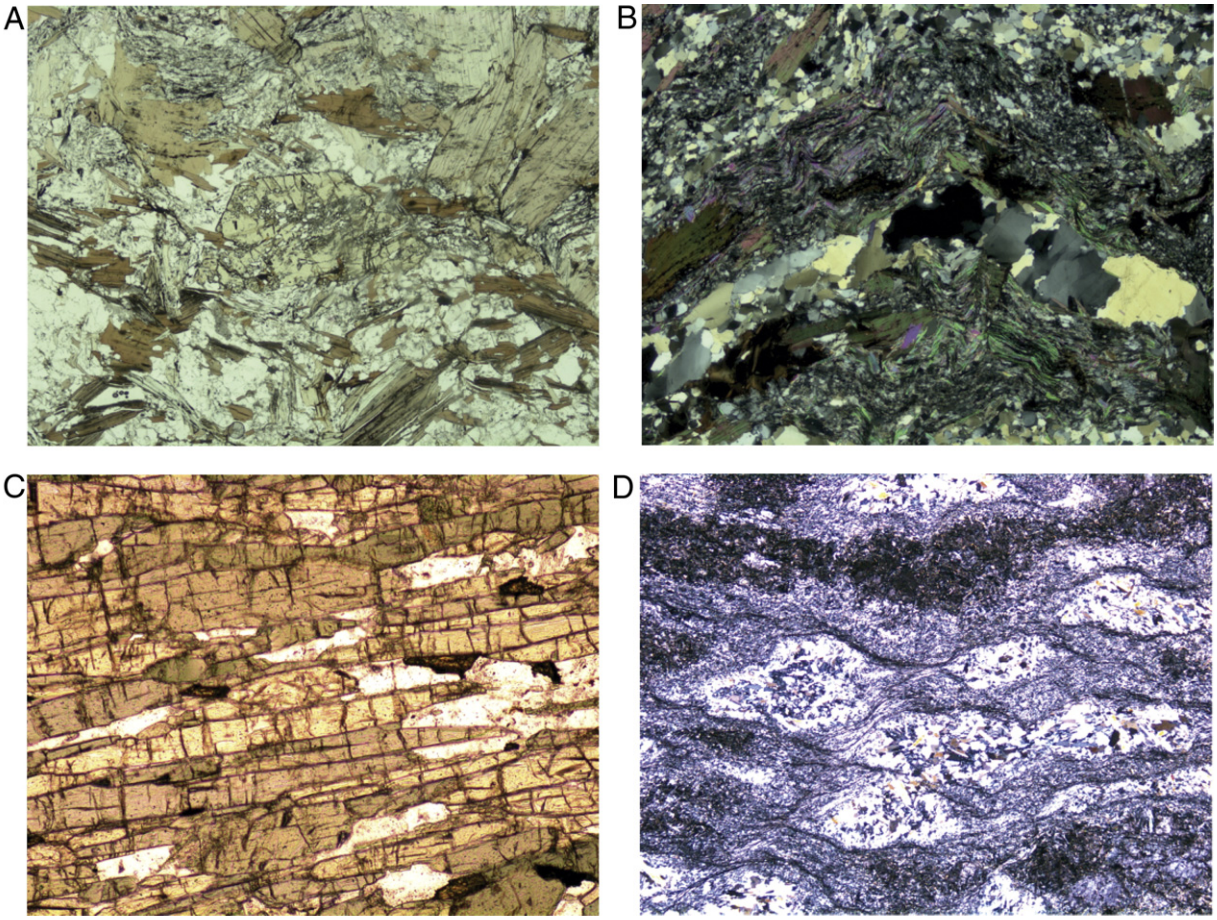

Fig. 10. Photomicrographs of representative Lolotoi Complex samples. A) Garnet–mica schist with disrupted foliation and two episodes of biotite growth. B) Quartz–mica schist with bands of quartz and fine-grained muscovite. Muscovite rich domains exhibit two different scales of folding. C) Amphibolite with quartz. D) Mylonitic quartz–mica schist. Extensive grain size reduction has occurred and a weak S–C mylonitic fabric is visible.

(Roosmawati and Harris, 2009-this issue) and coral terraces (Cox et al., 2006). Uplifted synorogenic units in central Timor also document the initiation of clastic sedimentation at around 2–3 Ma (Audley-Charles, 1986).

8.4. Summary

Various types of age determinations constrain the tectonic history of the Mutis and Lolotoi Complex by indicating that: 1) deposition occurred mainly after 80 Ma as indicated by detrital zircon grains near this age found in deep structural levels of the metamorphic Complex; 2) peak metamorphic conditions were reached near 45 Ma as indicated by Lu–Hf garnet ages; 3) rapid exhumation and cooling occurred from around 39 to 23 Ma as indicated by $^{40}Ar/^{39}Ar$ and apatite fission track thermochronology and a Late Oligocene unconformity; 4) shallow reburial beneath accumulating volcanic and sedimentary cover units to depths of the fission track partial annealing zone (4–5 km) occurred from 28 Ma to 3 Ma; and 5) uplift and emergence from a forearc basement position to high-level thrust nappes initiated at around 3 Ma due to collision with the Australian continental margin as indicated by the age of the first synorogenic sediment with metamorphic rock fragments.

These age constraints indicate that the Banda Terrane, which is now intercalated with Australian continental margin units, yields cooling ages that pre-date its collision with Australia by 23–46 Ma. The only affect of the Banda Orogen on these rocks is uplift and exhumation, not metamorphism as suggested originally by Hamilton (1979) and more recently by Kaneko et al. (2007). These results also suggest caution in using ages of metamorphism or metamorphic cooling to constrain the age of collision in older orogens with less temporal resolution than the active Banda Orogen.

9. Differences between the Aileu and Lolotoi metamorphic complexes of Timor Leste

In a recent synthesis of metamorphic rocks of the Banda Arc (Kaneko et al., 2007), the Aileu Complex of well-documented Australian affinity is lumped with the Asian affinity Lolotoi/Mutis Complex, and named the Timor–Tanimbar metamorphic unit. However, the Aileu Complex differs from the Lolotoi Complex in many significant ways.

The Aileu Complex of Audley-Charles (1968) is found along the north coast of Timor and some forearc ridge islands to the east of Timor. It rapidly decreases in metamorphic grade southward from amphibolite facies psammitic and mafic units near the coast to a phyllite and slate belt that inter-fingers with the Permian to Triassic Maubisse Formation of the Gondwana Sequence (Barber and Audley-Charles, 1976; Prasetyadi and Harris, 1996). The structure of the Aileu is characterized by a very distinct layer and foliation parallel shortening that forms a layer normal cleavage and foliation (Prasetyadi and Harris, 1996).

In contrast, the Lolotoi/Mutis Complex consists of metamorphosed Late Cretaceous to Tertiary arc-related units, with Eocene to Miocene Asian-affinity volcanic and sedimentary cover. Its structure is characterized mostly by layer normal shortening associated with extensional deformation. Detrital zircon age distributions in the Aileu and Lolotoi/Mutis Complexes are completely different (Harris, 2006). No zircon grains younger than Permian are found in the Aileu Complex (Harris, 2006) versus grains as young as 82 Ma in the Lolotoi Complex

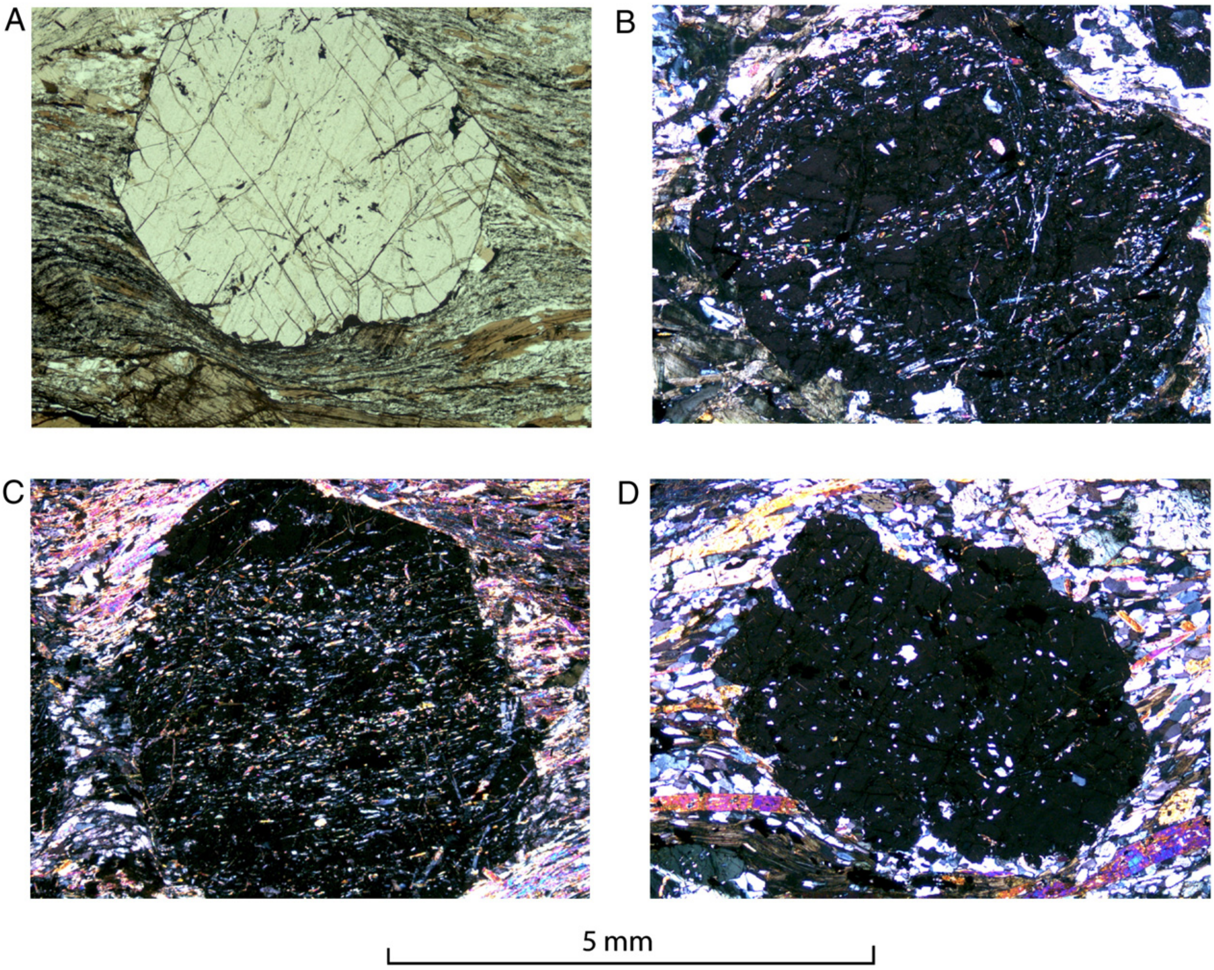

Fig. 11. Garnet photomicrographs. A) A nearly idioblastic garnet with strait inclusion trails, and bending and truncation of mica (sample 04T-MLO). B) Various episodes of garnet growth involving inclusion free areas surrounded by inclusion trails (sample 8-11-5). C) Pre-existing fabric (S_1) encased in garnet that is slightly oblique to, and finer-grained than external fabric (S_2) (sample SF-2). D) Resorbed garnet with quartz and mica inclusions showing no preferred orientation (sample 8-3-5).

(see above). One of the most important distinctions is difference in metamorphic cooling ages. The Aileu Complex yields Late Miocene to Early Pliocene $^{40}Ar/^{39}Ar$ metamorphic cooling ages (Berry and McDougall, 1986), whereas the Lolotoi Complex has a metamorphic age of 46 Ma and $^{40}Ar/^{39}Ar$ cooling ages of from 39–35 Ma. The metamorphic complexes were also exhumed at different times. Fission tracks in apatite grains in the Aileu complex are highly to completely annealed, indicating an exhumation age of <2 Ma (Harris et al., 2000), whereas the Lolotoi/Mutis Complex is overlain by an Oligocene unconformity and has apatite grains with model ages of >23 Ma. These metamorphic complexes clearly have different origins, metamorphic histories and pre- and syn-collisional relations to the Banda Arc and tell different parts of the story of its origin.

10. Sedimentary and volcanic cover

In many places the Lolotoi Complex is closely associated with volcanic and sedimentary units that correlate with those originally described unconformably overlying the Mutis Complex of West Timor (e.g. Tappenbeck, 1939), and in several other parts of the Banda Sea region, such as Sumba and Sulawesi (Harris, 2006). These units were first recognized in Timor Leste by Gageonnet and Lemoine (1958) on the southern part of the Bebe Susu Nappe near Same. Later, Carter et al. (1976) correlated these occurrences with the Palelo Group of West Timor based on distinctive successions of high-energy, shallow water siliciclastic units, Nummulites-bearing carbonate and associated silicic volcanic rocks.

During our field investigation of the Lolotoi Complex, we found many of the closely associated sedimentary and volcanic cover units described for the Mutis Complex in West Timor, such as the Cretaceous Palelo Group, Paleogene Metan Formation, Oligocene to Miocene Cablac Limestone and possibly the Pliocene Manamas Volcanics. Most of these occurrences are found on the fringes of the Lolotoi Nappe, central and southern portions of the Bebe Susu Nappe, eastern fringe of the Lacluta Nappe, and extensively throughout the Mata Bia Nappe (Harris, 2006).

We conducted two traverses through the cover units of the Lolotoi Complex along the Mota (river) Sui and Caraulun east of Same village on the southern edge of the Bebe Susu Nappe (Fig. 4C). These rivers flow to the south, and expose a fault-bounded section of mostly sedimentary rocks that are juxtaposed against the Lolotoi Complex to the north and mélange to the south. The fault contact with the Lolotoi Complex to the north consists of a damage zone hundreds of meters wide with several crosscutting shear fractures. The fault zone juxtaposes broken and structurally intercalated Lolotoi Complex units of black phyllite, and graphitic and choritic schist intruded by mafic and felsic dikes against sedimentary and volcanic units of the Noni Formation (Fig. 2). The sense of shear of the fault is ambiguous due to the multiply deformed nature of the units and poor exposure. Lack of mode 2 fractures restricts the possibilities of shear sense to either deep structural level Lolotoi metamorphic units thrust over its cover, or high structural level cover units normal faulted down over the Lolotoi Complex. We prefer the later interpretation based on the recognition of many late-stage extensional features (see below).

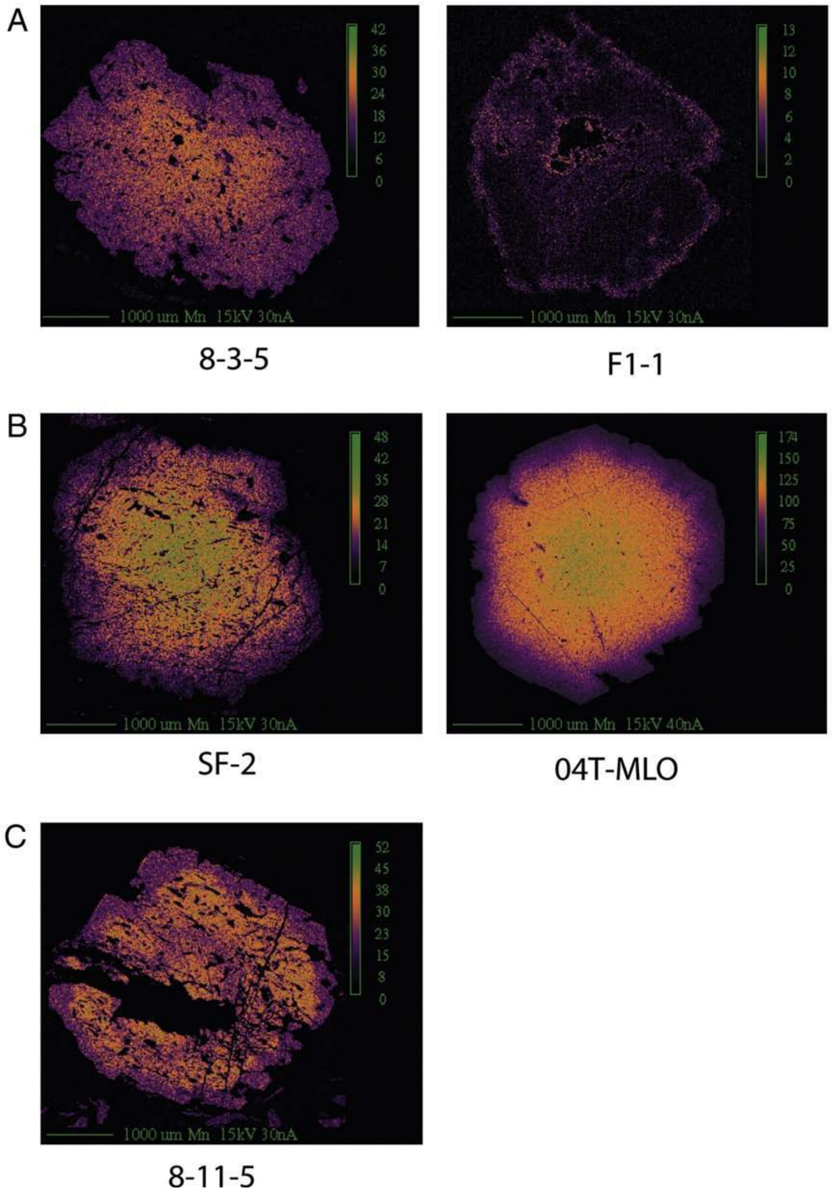

Fig. 12. Microprobe X-ray dot maps showing manganese zoning in garnet from garnet–mica schist. Most garnet grains show a single generation of growth with normal patters of Mn and Ca decreasing in abundance from core to rim, and Fe and Mg increasing from core to rim (A). Several samples show Mn-rich rims indicative of retrograde net transfer reactions (B). Only one garnet exhibits two episodes of growth, with a Mn peak near the center, and another Mn peak near the rim (C).

Noni Formation units in the Mota Sui, mostly consist of interbedded chert and tuff. Chert at the base of the Noni Formation in West Timor yields Aptian–Turonian radiolaria (Haile et al., 1979). In the Mota Caraulun, a massive cobble to boulder conglomerate over a hundred meters thick is found at the base of the cover succession in fault contact with the Lolotoi Complex. Clasts in the conglomerate include intermediate volcanic rocks, gabbro/diorite, red and black chert, quartz, shale, sandstone, chloritic and graphitic low-grade metamorphic units, quartz–mica ± garnet schist and gneiss. One of the andesite cobbles yields a zircon U/Pb age of 83 ± 2 Ma (Harris, 2006). This result provides a maximum age constraint for the conglomerate, which is slightly younger than the chert units. This age is similar to the youngest detrital zircon grains found in the Lolotoi Complex immediately underlying the conglomerate.

In West Timor a similar unit is found at the base of the Haulasi Formation, which also includes Late Cretaceous turbidites and Paleogene tuff and lava deposits. Poorly exposed sections of these units are found further downstream (upsection) from the conglomerate. The lower turbidite sections are more distal and well-indurated than those higher in the section, which feature wood and leaf fossils.

Overlying the turbiditic section are the Eocene Dartollu Limestone and Oligocene Barique Formation of Audley-Charles (1968). These units are very distinctive from anything found in equivalent age units of Australian affinity (Fig. 2). An E–W trending ridge of steeply south dipping Dartollu Limestone crosses both the Mota Sui and Caraulun. It consists of a microfaunal assemblage of large foraminifera that are characteristic of a fossil assemblage only found in Sundaland and on low latitude Pacific islands (Lunt, 2003), which eliminates the possibility of these sedimentary units forming parts of the Australian continental margin.

The Barique Formation consists of intermediate composition volcanic flows and tuffs interbedded with limestone and sandstone. The parts of this unit that we analyzed has arc-related geochemical affinities (Appendix A, Fig. 7), which demonstrate that the Lolotoi Complex was near, if not part of, a volcanic arc during the Oligocene. It

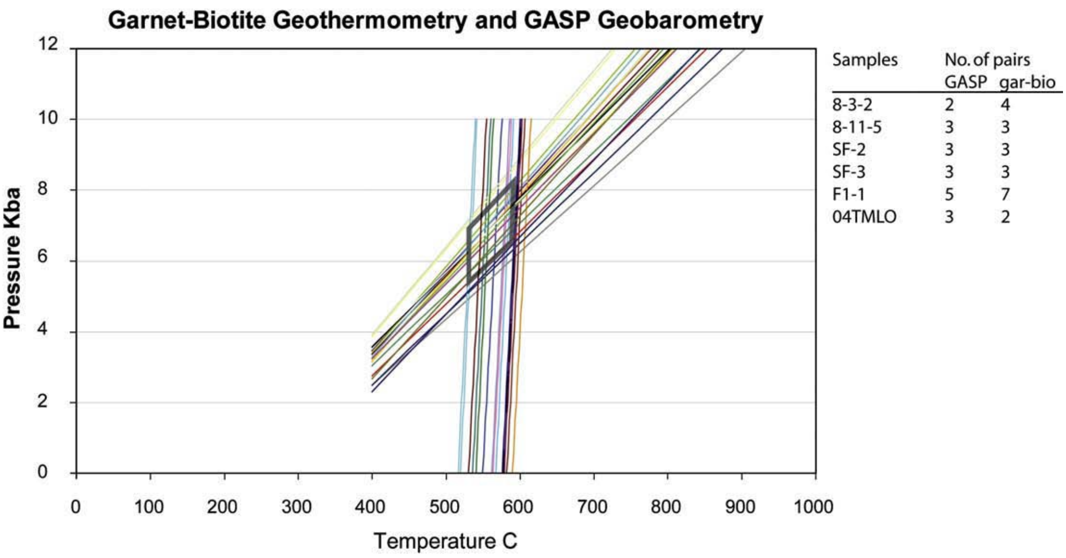

Fig. 13. Geothermobarometric plot of garnet–biotite thermometers (Kleemann and Reinhardt, 1994) and garnet–aluminosilicate–quartz–plagioclase (GASP) barometers (Newton and Haselton, 1981). The grey diamond provides the range of results. Variation within each samples is minimal.

is also during this time that the Lolotoi Complex experienced peak metamorphism followed by rapid exhumation.

The exhumation of the Lolotoi and Palelo Group is well documented throughout Timor by a Late Oligocene unconformity first described by T'Hoen and van Es (1926). The unconformity is overlain by the Cablac Limestone, which is named after late Oligocene limestone found at the base of Mt. Cablac in the eastern most part of the Bebe Susu nappe. A basal conglomerate above the unconformity is well preserved near the base of Mata Bia in the eastern part of Timor Leste (Fig. 6F) and consists of clasts from older Banda Terrane units embedded in a carbonate matrix. Clast types are very similar to the conglomerates of the Haulassi Formation, with the exception of *poly*metamorphic pelitic schist, intermediate composition plutonic rocks, Eocene *Nummulites* fragments and large Oligocene foraminifera. The conglomerate is depositionally overlain by massive calcilutite with Late Oligocene foraminifera (Audley-Charles and Carter, 1972) and Middle Miocene marl and ash units (Carter et al., 1976). There are several large carbonate build-ups associated with the Cablac Limestone in Timor Leste, which form parts of the Cablac Range of the Bebe Susu nappe, Bibiliu Range of the Lacluta nappe and Mata Bia (Fig. 2B).

The youngest Banda Terrane cover units are found locally on the north coast of Timor, and are part of the Pliocene Manamas Volcanics, which include the Ocussi volcanic pile (Fig. 2B). However, during our investigation, we discovered a large occurrence of pillow basalt on the north coast of Timor Leste near Baucau that may be the equivalent of the Ocussi Volcanics. It consists of a basaltic andesite with arc-related trace element signatures (Appendix A) that are very similar to those found in the Ocussi volcanic pile (Harris, 1992).

10.1. Discussion

Sedimentary and volcanic cover units of the Cretaceous Palelo Group and Paleogene Metan Formation are interpreted as deposited unconformably over the Lolotoi and Mutis Complexes. However, the age of peak metamorphism and cooling of the metamorphic rocks is younger than the age of these unmetamorphosed 'overlying' units. This age conflict raises important additional questions about the

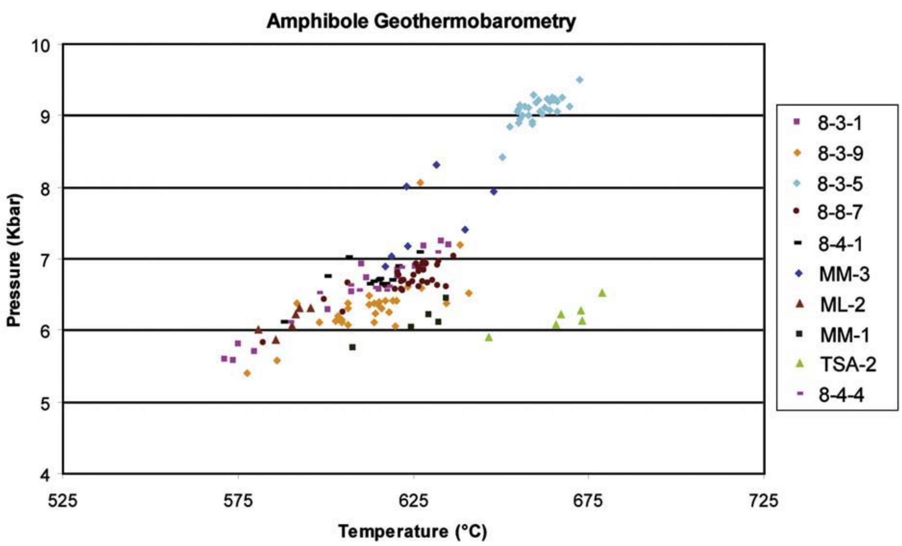

Fig. 14. Geothermobarometry of amphibole grains (based on Gerya et al., 1997). Most samples have temperatures ranging from 580 °C to 640 °C, though some are slightly higher. Pressures range mainly from 6–8 kbars. However, one float sample has amphiboles that plot between 9 and 10 kbars.

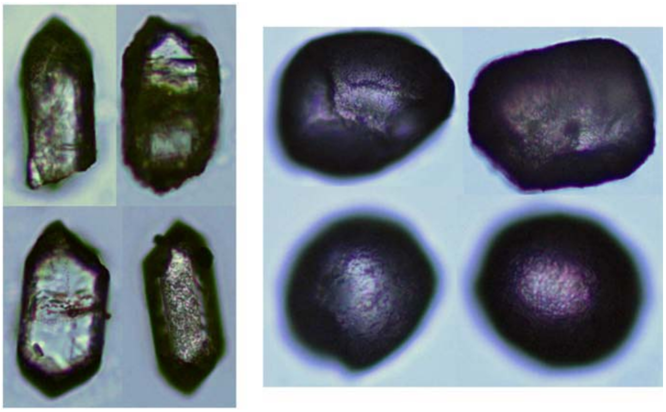

Fig. 15. Detrital zircons of Late Cretaceous age (left) and Late Precambrian age (right).

metamorphic history of the Lolotoi and Mutis Complexes. For example, Cretaceous conglomerate in the Palelo Group contains metamorphic clasts very similar in composition and metamorphic grade to the immediately underlying Lolotoi/Mutis Complex. It has always been assumed that these clasts were derived from the metamorphic rocks immediately beneath them, which requires an age of >83 Ma for the Lolotoi/Mutis Complex.

To resolve this conundrum. We infer that large amounts of extension have taken place along the boundary between the Palelo Group and the Lolotoi/Mutis Complex, which can explain metamorphic rocks younger than its structurally overlying cover. Extension is the rule rather than the exception in arc terranes. Many examples of extensionally collapsed arcs are now reported from marginal basins of the western Pacific region. Like the Banda Sea Basin, these remnant arc ridges are commonly embedded in oceanic lithosphere younger than

Table 3
U/Pb age of sample 8-3-9.

Sample name	207/235 age	1 sigma abs err	206/238 age	1 sigma abs err	207/206 age	1 sigma abs err
CES839_01a	97.2	3.2	81.8	2.3	519.8	34.4
CES839_02a	150.4	7.6	116.0	5.5	759.4	43.5
CES839_03a	87.6	3.4	86.5	2.7	143.9	48.2
CES839_04a	761.8	19.0	674.7	19.5	1050.9	28.6
CES839_05a	106.6	3.7	83.9	2.5	677.1	35.5
CES839_06a	597.8	14.7	589.4	16.6	655.6	21.3
CES839_07a	635.4	15.3	609.9	17.2	752.8	19.7
CES839A_02a	278.0	4.9	242.7	3.3	602.7	27.2
CES839A_03a	124.9	2.4	113.8	1.6	358.7	27.7
CES839A_04a	385.8	6.6	325.5	4.7	780.7	25.9
CES839A_06a	123.5	2.5	93.5	1.3	765.6	28.6
CES839A_06b	147.7	3.1	100.5	1.4	1008.8	31.1
CES839A_07a	92.1	1.7	88.0	1.3	218.0	23.1
CES839A_07b	86.5	1.6	83.3	1.3	191.2	23.5
CES839A_08a	108.8	3.7	112.9	2.2	35.5	63.5
CES839A_08b	174.6	6.5	127.6	2.7	885.3	62.7
CES839A_10a	1866.2	15.5	1696.3	24.2	2074.0	10.8
CES839A_11a	722.2	10.2	679.6	9.7	872.0	22.5
CES839A_13a	657.2	7.4	651.3	8.2	693.0	11.7
CES839A_14a	611.8	8.4	590.9	8.9	705.1	15.4
CES839A_15a	267.9	4.6	236.6	3.6	567.8	20.8
CES839A_16a	118.2	2.9	96.1	1.5	606.9	38.3
CES839A_17a	122.3	2.9	92.0	1.6	776.4	31.4
CES839A_18a	479.3	7.5	443.6	6.6	669.2	22.0
CES839A_19a	1123.8	13.2	1097.9	16.8	1188.6	15.5
CES839A_21a	641.0	8.9	611.4	9.7	762.0	13.7
CES839A_23A	121.4	3.1	109.5	1.8	377.2	42.2
CES839B_25A	101.2	3.0	90.1	1.5	387.2	51.9
CES839B_26A	1490.7	24.7	1316.9	36.7	1760.7	9.7
CES839B_27A	736.3	7.8	722.3	8.7	794.3	11.7
CES839B_28A	98.9	1.9	85.0	1.2	465.1	27.9
CES839B_30A	123.8	3.5	88.0	1.5	895.9	44.4

Table 4
^{176}Lu/^{176}Hf age analyses.

Sample	Type	^{176}Lu/^{177}Hf	2σ abs	^{176}Hf/^{177}Hf	2σ abs	Lu ppm	Hf ppm
8-3-2							
8-3-2 C.1	Garnet clean	3.52123	0.00704	0.285853	0.000009	5.610	0.226
8-3-2 U1.1	Garnet less clean	3.57296	0.00715	0.285868	0.000010	4.573	0.182
8-3-2 U2.1	Garnet less clean	2.84393	0.00569	0.285315	0.000007	5.208	0.260
8-3-2 U3.2	Garnet less clean	1.48191	0.00296	0.284101	0.000006	4.717	0.452
8-3-2 WR.1	Sav whole rock	0.02499	0.00005	0.282811	0.000006	0.198	1.124
8-3-2 WRB.1	Bomb whole rock	0.00792	0.00002	0.282807	0.000006	0.262	4.697
8-3-5							
8-3-5 C.1	Garnet clean	4.03088	0.00806	0.286517	0.000021	3.084	0.109
8-3-5 U1.1	Garnet less clean	4.09187	0.00818	0.286610	0.000034	2.859	0.099
8-3-5 U2.1	Garnet less clean	4.41653	0.00883	0.286845	0.000018	3.004	0.097
8-3-2 WR.1	Sav whole rock	0.12201	0.00024	0.283206	0.000008	0.339	0.394
8-3-2 WR.B1	Bomb whole rock	0.02282	0.00005	0.283146	0.000006	0.383	2.379
O4TMLO							
O4TMLO C.1	Garnet clean	20.21426	0.04050	0.301189	0.000054	17.899	0.126
O4TMLO U1.1	Garnet less clean	15.84595	0.03175	0.300938	0.000072	13.479	0.121
O4TMLO U2.1	Garnet less clean	11.42500	0.02300	0.292602	0.000030	12.306	0.153
O4TMLO WR1.1	Sav whole rock	0.01828	0.00004	0.282750	0.000019	0.011	0.086
O4TMLO WR2.1	Sav whole rock	0.01598	0.00003	0.281818	0.000043	0.015	0.134
O4TMLO WRB2.1	Bomb whole rock	0.00522	0.00001	0.282681	0.000006	0.025	0.041
SF-2							
SF-2 C.1	Garnet clean	3.76012	0.00752	0.286398	0.000048	3.246	0.123
SF-2 U1.1	Garnet less clean	3.52681	0.00705	0.286546	0.000179	1.958	0.079
SF-2 U2.1	Garnet less clean	2.99564	0.00599	0.285383	0.000024	3.779	0.179
SF-2 WR.1	Sav whole rock	0.01951	0.00004	0.282848	0.000006	0.186	1.351
SF-2 WRB.1	Bomb whole rock	0.00941	0.00002	0.282862	0.000006	0.270	4.065

the arc. The occurrence of multiple volcanogenic turbidite successions, carbonate and volcanic units of the Palelo Group and other units now found in fault contact with the Lolotoi/Mutis Complex is consistent with an intra-arc extensional setting.

11. Structural analysis

Previous studies have investigated various phases of deformation recorded in Metamorphic units of the Mutis Complex (e.g. Earle, 1980; Sopaheluwaken, 1990), but the structure of the Lolotoi Complex is unknown. From the Mutis massif in West Timor Brown and Earle (1983) describe deformation sequences for both mono- and poly-deformed metamorphic rocks that consist of a compound S_1 foliation (D_1) followed by transposition of S_1 to S_2 (D_2), which is axial planar to tight isoclinal folds of F_2. The origin of these deformation phases is not discussed. D_2 is followed by two phases of open F_3 (D_3) and F_4 (D_4) folds with hinge-lines trending E–W. Thrust faults with generally southward movement may produce D_3 and D_4 folds. They state that most of these structures are cut by late stage normal faults (D_5). Other Mutis complex massifs have similar structural orientations (Fig. 19D). We conducted a structural analysis of the Bebe Susu and Lolotoi nappes in order to test if the Lolotoi Complex shares a similar

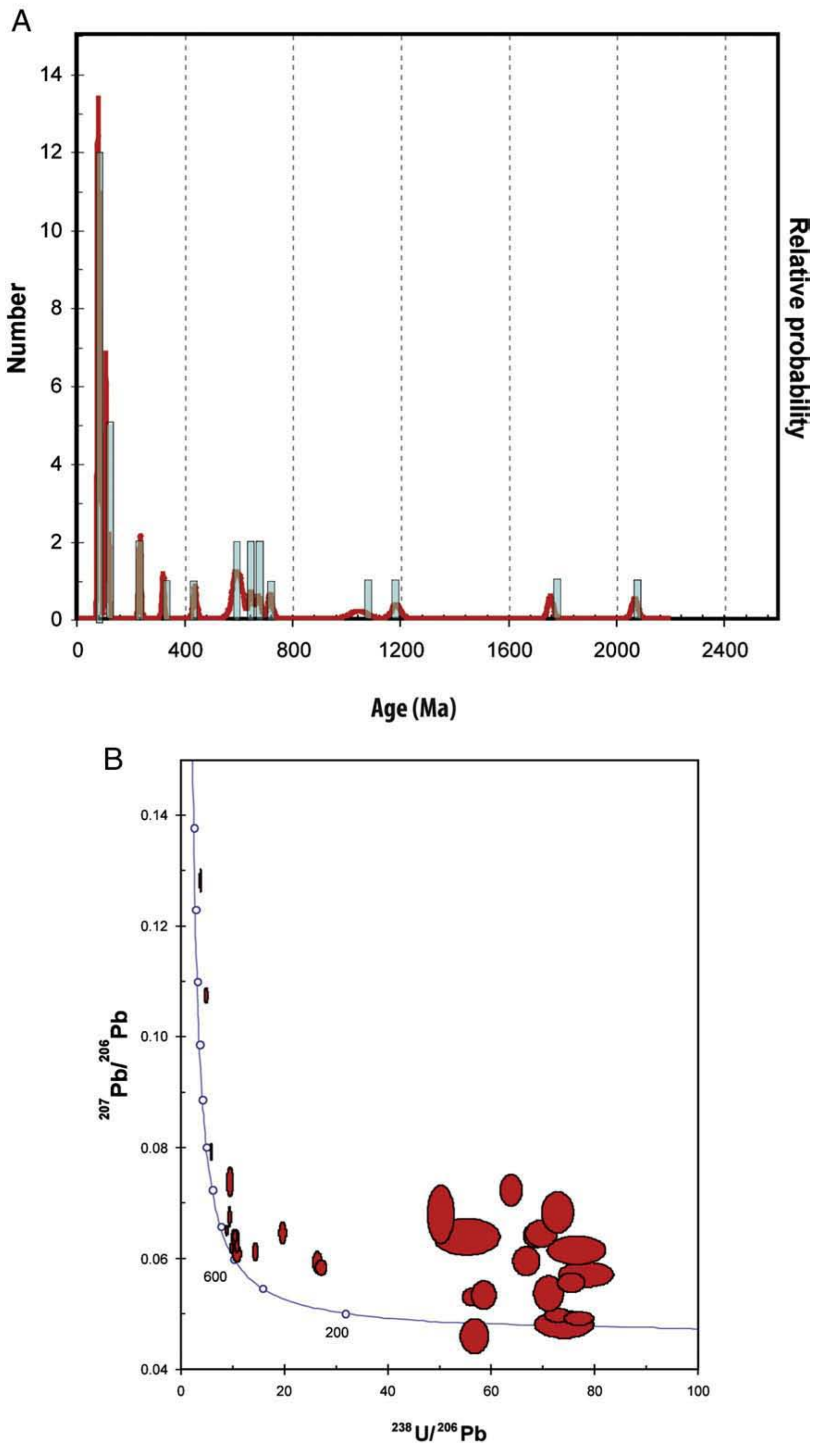

Fig. 16. U/Pb age analysis of detrital zircon grains from a garnet amphibolite of the Lolotoi Complex. A) Histogram of ages and relative probability with major spikes at 87 Ma and 120 Ma, minor spikes at 239 Ma and 663 Ma. B) Age distribution on a U/Pb concordia curve.

structural history to the Mutis Complex, and relate deformational features to known tectonic events in the region.

11.1. Foliation and folding

Structural mapping of the Lolotoi Complex reveals a major foliation that is rarely steeply dipping and parallel to finely laminated compositional layers (Fig. 6A–C). These layers commonly have multiple generations of folds and some mylonitic textures. Locally, a second foliation is seen in outcrop that is parallel to fold axial surfaces (Fig. 6C). In the field, we referred to the earliest foliation as a composite S_0–S_1, which is associated with recumbent isoclinal folds, F1 (Fig. 6A). The second foliation (S_2) we relate in the field to F_2 (Figs. 6B and C).

In thin section (Fig. 11) compositional layers are as thin as a few millimeters and consist mostly of aligned biotite, white mica and stretched quartz. The foliation surrounds relatively inclusion free garnet (Fig. 11A) that has $^{176}Lu/^{176}$ Hf age determinations of 45–46 ± 3 Ma. These textural relations suggest that relatively inclusion free

Table 5
Apatite fission-track data.

Sample	Fossil tacks	Induced tacks	Total mica counts	Age (Ma)	Error (1st std dev.)	Notes
FC	270	685	2667	34.62	2.58	Standard
LC	97	630	2667	13.54	1.50	Standard
MT 43	178	779	2667	20.08	1.71	From Kisar Island
MT 44	177	859	2667	18.12	1.54	From Kisar Island
MT 45-1	109	760	2667	12.62	1.32	From Kisar Island
MT 112-91	16	34	2667	41.32	12.55	Mutis Massif
MT 105-91	Track length data only		–	–	–	Usu Massif

garnet porphyroblasts grew before a foliation developed, and are therefore pre-kinematic.

Some garnet porphyroblasts overgrow a foliation that is manifest as inclusion trails generally finer grained and slightly oblique to foliation surrounding the garnet (Fig. 11B and C). We interpret these garnet porphyroblasts as syn-kinematic due to the fact that they most likely grew during the early development of foliation when the rock was less recrystallized. Some garnet porphyroblasts even have inclusions with no preferred orientation (Fig. 11D), which may represent the earliest phases of recrystalliztion, but still pre-kinematic growth.

The possibility exists that these and even relatively inclusion free garnet porphyroblasts may have originally grown over a foliation that was resorbed during garnet growth. However, the closely spaced fine-grained nature of the included grains cannot represent the remnants of originally larger, resorbed inclusions.

Differences in orientation and grain size between early-formed foliations included in garnet porphyroblasts and the major foliation that encloses them require a slight modification to the structural evolution observable in outcrop. The earliest fine-grained foliation-forming inclusion trails in garnet porphyroblasts we interpret as S_1 and associate it with deformation phase, D_1. Most inclusion trails show little to no folding, suggesting that D_1 is associated with layer-normal stresses. Since garnet growth is prograde (see above), S_1 records a phase of deformation that predates peak metamorphism.

The foliation enclosing the garnet porphyroblasts, which is the main foliation found in outcrop and in thin section, we interpret as a composite S_0–S_1–S_2, which is due to transposition during the development of isoclinal recumbent folds (F1). The hinges of these folds are locally found completely detached from their limbs (Fig. 6A and B). We associate this phase of vertical shortening with D_2.

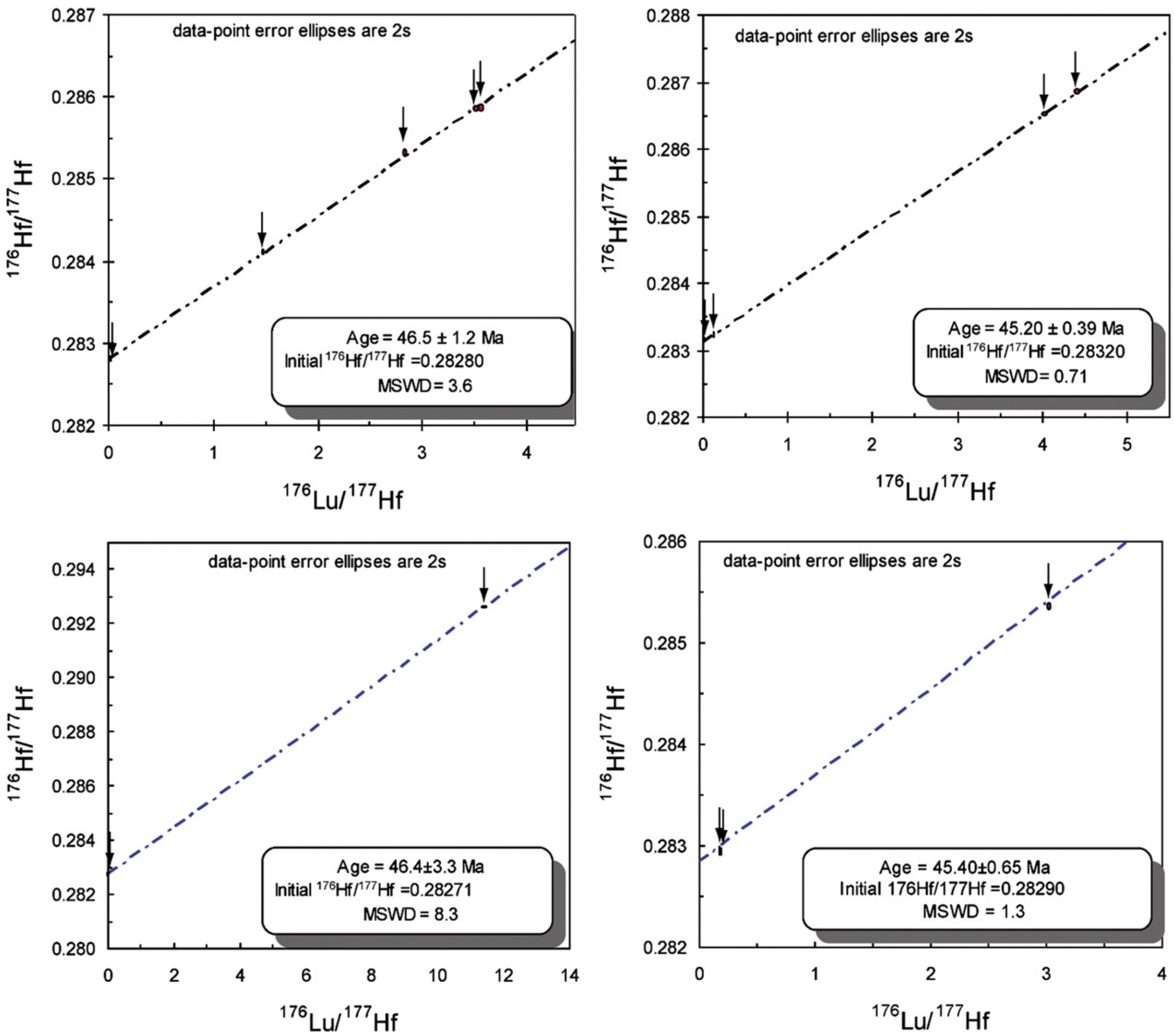

Fig. 17. Lutetium–Hafnium isochrons for four samples of garnet from the Lolotoi Complex. Multiple points on the isochron were obtained by analyzing clean garnet, unclean garnet, and whole rock fractions. Data point error ellipses are 2σ.

D_2 isoclinal recumbent folds (F1) are locally refolded into a series of micro to mesoscale asymmetrical folds (F_2) with mostly top to the SE fold asymmetry (Fig. 6B and C). A second foliation (S_3) is found locally parallel to axial surfaces of F_2 folds in some pelitic units (Fig. 6C). These features indicate a phase of layer-parallel shortening (D_3) that is similar in style and geometry to fault-related folds observed also in the Cretaceous to Eocene sedimentary and volcanic cover units of the Lolotoi Complex (Fig. 6D), and in structurally underlying Australian continental margin units.

These different deformation phases cause considerable spatial variation in foliation attitude throughout the Lolotoi Complex. However, in geometric space poles to S_2 cluster along a Pi-girdle trending NW–SE with a Pi-pole that slightly plunges to the SW (Fig. 19A and B). The Pi-pole is sub-parallel to F_2 fold hinge-lines (Fig. 19C), and indicates most foliation is folded along a NE–SW axis. There is also a subsidiary set of folds that trend NW–SE (Fig. 19C). Localized mesoscale folds with large dip domains are also observed. These structures are open (inter-limb angle 60°–120°) and have mostly SE verging asymmetry and NE–SW trending hinge-lines with little to no plunge, which is also characteristic of F_2 (Fig. 19C).

We found that the Lolotoi Complex records all of the deformational events reported from the Mutis Complex. The only difference in our interpretation is that we relate most normal faulting to Late Eocene extensional exhumation of metamorphic complexes. To further test geometrical similarities we compiled all of the previously published measurements of S_2 foliation planes available for the Mutis Complex (Tappenbeck, 1939; Earle, 1980), which includes many of our own measurements from the Mutis, Miomoffo, Usu and Lakaan Massifs (Fig. 19D). The resulting Pi-girdle of poles to S_2 foliation has a nearly identical trend to that of poles to S_2 foliation of the Bebe Susu and Lolotoi Massifs of Timor Leste (Fig. 19E).

11.2. Brittle deformation

The Lolotoi Complex and its sedimentary and volcanic cover are deformed by both normal and reverse faults. The absolute age of these structures is unknown except for the fact that some faults are truncated by the Oligocene unconformity. There are also cross cutting relations that generally favor normal faulting (Fig. 6E) prior to late stage thrusting (Fig. 19C), although many exceptions are found.

Most garnet porphyroblasts throughout the Lolotoi Complex have extensional fractures that are perpendicular to the composite S_0–S_1–S_2 foliation (Fig. 11A and B). Sometimes the fractures are filled with zeolite indicating they formed after the rocks had mostly cooled. Similar relations are found in outcrop where steeply dipping conjugate fractures are associated with vertical veins and normal faults with mainly top-down-to-the south and SE sense of shear (Fig. 19F and H). Geomorphic expressions of normal faulting are also observed, such as the contact between the Lolotoi Complex and its cover units along the southern edge of the Bebe Susu Nappe (Fig. 4C).

Thrust faults exhibit two dominant orientations: one strikes NE–SW with movement dominantly to the SE, the other set strikes NW–SE with movement both to the SW and NE (Fig. 19G). These structures are similar to the two sets of F_2 hinge-lines (Fig. 19C). One thrust fault offsets river gravels, which is consistent with ongoing thrust-related seismic activity.

We infer that normal faulting accompanied extensional unroofing of the Lolotoi Complex, and is associated with D_2. However, D_2 cannot account for all normal faults observed as some obviously are post Late Miocene to Pliocene nappe emplacement. Thrust faults show a geometric affinity with D_3. If this is the case, then D_{1-2} is associated with extensional collapse of the Great Indonesian Arc before Oligocene time, and D_3 is associated with Late Miocene to present collisional deformation.

11.3. Discussion

Syn-metamorphic extensional exhumation of the Lolotoi Complex is consistent with the common occurrence of the same in Sulawesi (van Leeuwen, 1981), detached continental crustal fragments within the Banda Sea Basin (Honthaas et al., 1998) and the western Mutis Complex (Brown and Earle, 1983), which has decompressional growth of cordierite and sillimanite at $t=700°$ and $P=5$ kbar). These areas were likely closer to the arc than the eastern Mutis and Lolotoi Complexes, which did not experiences these high temperatures. However, D_{1-2} structural features of the Lolotoi Complex provide evidence for an early decompressional deformation phase with a vertical maximum stress and pure shear deformational modes during Late Eocene growth of garnet.

Nearly 40 million years after these events the Lolotoi Complex collided with the Australian continental margin causing layer-parallel shortening, which we associate with D_3. The accretion process includes thrust-related folding that deformed the Banda Terrane roof-thrust along with structurally underlying Australian continental margin units. The basal thrust of the Mutis and Lolotoi Complex nappes is also folded due to post-emplacement thrust duplexing of structurally underlying units. The duplex zones form NE–SW trending structural culminations throughout Timor (Harris et al., 2000) that warp the basal thrust of the nappes so they tilt either NW or SE. On the forelimb of the Aitutu Anticline the basal thrust of the Bebe Susu Nappe is tilted up to 40° SE (Fig. 4B). The

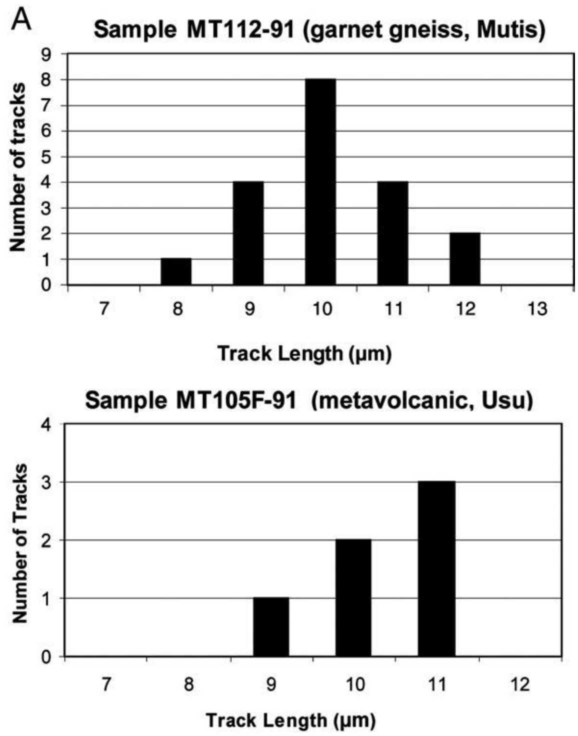

Fig. 18. Apatite fission-track age results. A) Histogram of horizontal apatite fission track lengths for a sample from the Mutis Massif and Usu Massif. Lack of complete 16–18 µm tracks indicates some annealing has occurred and samples have been exhumed from the partial annealing zone recently enough that no new horizontal tracks are detected. B) Apatite fission-track thermal history models using AFTsolve 0.8.3 (Ketcham et al., 2003). 1) Time–temperature plot of an inverse model that produced statistically the best fit to measured track length data. Geological constraints used in inverse modeling include a 45.36 Ma age of peak metamorphism at around 600 °C, a 28 Ma depositional age of overlying unmetamorphosed carbonate near 20 °C, and a recent collision related exhumation. 2) Inverse model that only uses beginning and end constraints and results in a statistically poor fit. 3) Forward modeled path that closely resembles the inverse model shown in A.

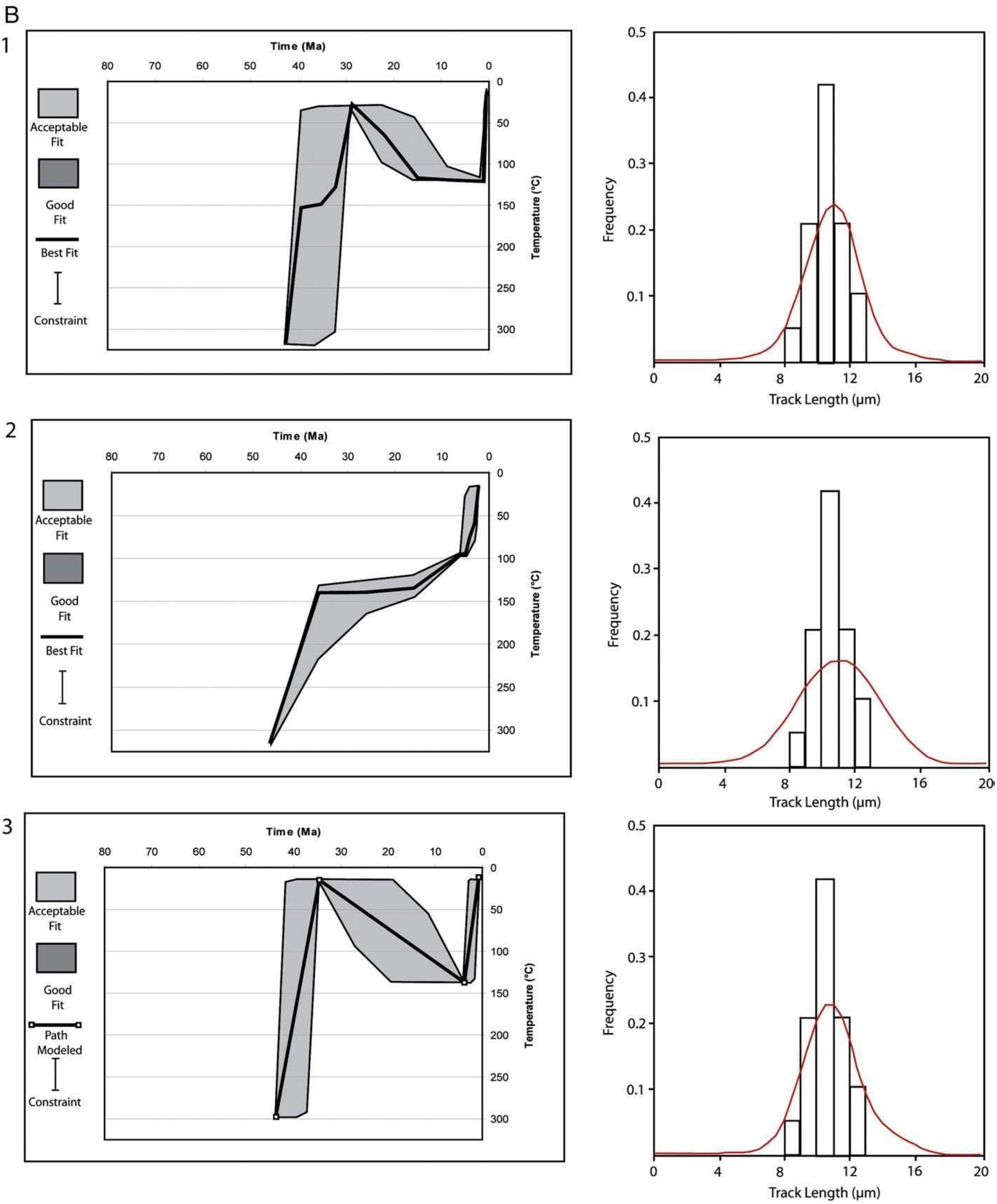

Fig. 18 (*continued*).

ongoing development of these large wavelength folds is responsible for the uplift of coral terraces along the north coast of the western and eastern most parts of Timor (Cox et al., 2006) and continued seismicity with thrust-related fault plane solutions.

11.4. Structural base of the Lolotoi nappe

Structurally underlying the Lolotoi Complex and some of its cover units is a tectonic mélange that transitions into fold and thrust

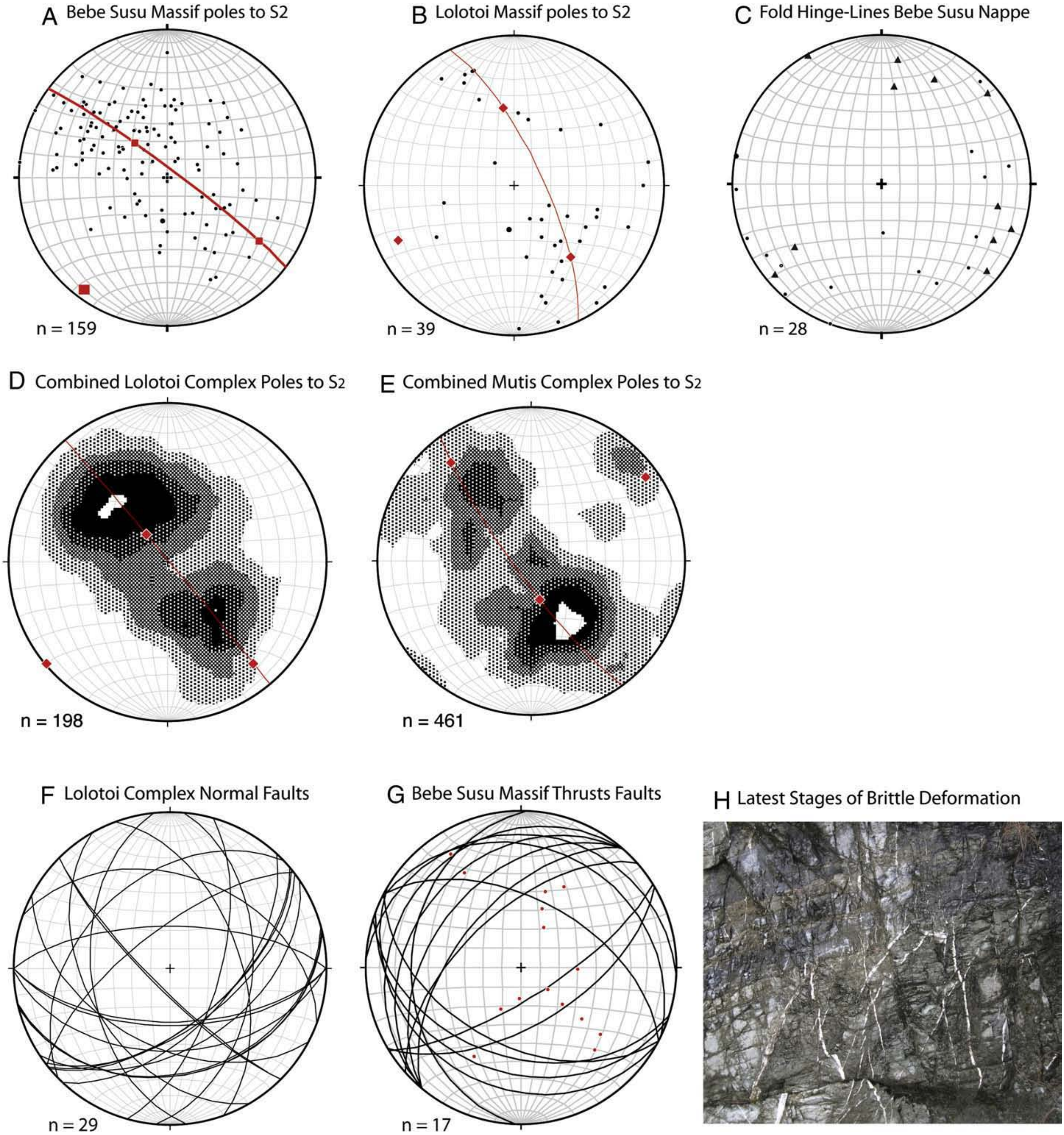

Fig. 19. Structural data from the Lolotoi and Mutis Complexes plotted on lower hemisphere equal-area stereographs using Stereonet 6. Poles to S_2 foliation with Pi-girdle and Pi-pole for the Bebe Susu Massif (A) and the Lolotoi Massif (B) indicating dominantly NE–SW fold hinge-lines associated with NW–SE $\sigma1$ and fold vergence. C) Trend and plunge of mesoscale fold hinge-lines (F_2). Triangles represent outcrop fold hinge-line measurements and dots represent fold axes calculated from mesoscale fold limb measurements. Contour of combined poles to S_2 foliation for the Lolotoi (D) and Mutis (E) Complexes. Mutis Complex data is from the Boi and Mollo Massifs (Earle, 1980; Tappenbeck, 1939, respectively), and the Mutis, Usu and Lakaan massifs (unpublished data from co-author). F) Photo of late stage extensional and conjugate fractures associated with a steep $\sigma1$ cut by a low-angle thrust fault.

cover units of the Australian continental margin. Mélange is characterized by mostly block-in-clay facies made of a highly mixed, and structurally modified array of blocks ranging up to broken thrust sheets of around 1 km^2 in areal extent. Near the base of the Banda Terrane nappes these blocks consist in downward stratigraphic order of fragments of the Lolotoi Complex and its sedimentary and volcanic cover, ultramafic units, alkali basalt and crinoidal limestone of the Maubisse Formation, and broken Gondwana Sequence units (Harris et al., 1998). Some of the best exposures of these units are on the SW edge of the Bebe Susu Nappe near the villages of Aitutu and Same, near the village of Laclubar, and on the northern side of Mata Bia.

The mélange records high shear strains in both its matrix and included blocks. The clay-rich matrix is strongly indurated with most faces representing slicken-sided surfaces. Although this fabric is common to mélanges, it is not evidence in and of itself of tectonic processes. However, the extent of shear strain is clearly demonstrated by the degree of block mixing and size reduction. Most blocks have high shear fracture and vein densities that are commonly in conjugate sets and consistent with cataclastic particle size reduction under high fluid pressures. Blocks of multiple generations of fault breccia are also found. The variety of juxtaposed block compositions, sizes and shapes also documents large amounts of slip and brittle shear processing (Harris et al., 1998).

In the northern portion of the Bebe Susu Nappe, blocks of pink, crinoidal limestone protrude from low-lying hills surrounded by non-resistant Lolotoi Complex graphitic and greenschist units (Fig. 4A). These blocks are mapped as part of the Permian Maubisse Formation by Audley-Charles (1968) and Grady and Berry (1977). However, the contact relations between the limestone units and the metamorphic units are interpreted in different ways. Audley-Charles (1968) shows them as thrust over the Lolotoi Complex. However, Chamalaun and Grady (1978) and later Charlton (2002) interpret the Permian units as in situ, and deposited on top of the Lolotoi Complex. This interpretation requires that the Lolotoi Complex is pre-Permian, which conflicts with data presented by Audley-Charles (1968) that it is overlain by Cretaceous to Miocene sedimentary and volcanic units, and age data presented here indicating a Late Cretaceous protolith and Eocene metamorphic age.

Our mapping of this region revealed a clearly exposed zone of mélange up to 30 m thick between the Permian limestone units and structurally overlying Lolotoi metamorphic units. Similar contact relations are also found directly to the southeast, and are traceable beneath the thin edge of the Bebe Susu Nappe. These structural relations demonstrate that the Permian limestone blocks are exposed in a fenster in the northern thin edge of the Bebe Susu Nappe. The fenster forms in a domed region of the basal thrust (Harris, 2006), and the resistance to erosion of limestone blocks within it enhances its geomorphic relief.

Gondwana sequence units structurally underlying the Banda Terrane exhibit similar low temperature deformational styles and transport directions to the metamorphic fabrics of the Banda Terrane (Harris et al., 2000). However, these different events are separated by around 40 my. It is likely that the orientation of the Great Indonesian Arc was similar to that of the current Banda Arc, and that emplacement related folding events overprint both the pre-existing structure of the Banda Terrane and Australian continental margin units.

11.5. Sequence of deformation

Overall, Banda Terrane massifs across both West and East Timor show consistent NE–SW striking foliation and fold hinge-lines, which implies little to no vertical-axis rotation has occurred between the various bodies. At least three main phases of deformation are recorded in the Lolotoi Complex. We infer that D_{1-2} is pre-Oligocene, and D_3 is latest Miocene to present.

D_{1-2}) Plastic mode layer perpendicular shortening (assuming bedding planes were near horizontal). S_1 foliation formed parallel to compositional layering (S0) due to vertical loading before peak metamorphism. The early S_1 foliation is fine-grained, rarely folded and is only preserved as inclusions in garnet sub-parallel to S_2. Hinges of isoclinally folded S_2 are found locally in thin-section and outcrop that demonstrate a vertical maximum stress forming high amplitude, short wavelength recumbent-style folds.

D_3) Plastic and brittle mode deformation folds composite S_2 into asymmetric micro-and meso-scale structures. Thrust fault related fold asymmetry demonstrates mostly SE vergence and in sedimentary and volcanic cover units, and structurally underlying accreted units of Australian affinity.

12. Conclusion

Petrologic analysis of Lolotoi metamorphic rocks indicates a mostly sedimentary origin with original deposition of inter-layered volcanogenic and pelitic sedimentary successions (shale-greywacke) and arc-related volcanic deposits (basaltic to basaltic andesite compositions). The sedimentary protolith of the Lolotoi Complex was deposited after 82 Ma, which is the youngest detrital zircon present in amphibolite within the core of the Bebe Susu Nappe.

Provenance data obtained from discriminant diagrams, based on major and trace element whole rock geochemistry, indicate mixed MORB and volcanic arc affinities for the igneous units and intermediate to mafic continental and oceanic arc sources for the sedimentary units. Volcanic and sedimentary protoliths are interpreted as proximal forearc basin deposits on the southern edge of the eastern Great Indonesian arc before it extended to form the Banda Sea floor and current Banda arc.

Metamorphism is attributed to processes occurring in the arcward part of a forearc basin, which include burial to depths of around 21–26 km and temperatures of 530 °C to 680 °C, which resulted in upper greenschist and amphibolite facies metamorphism. Peak metamorphism documented by Lu–Hf age analysis of garnet occurred at 45–46 Ma. Exhumation of the metamorphic rocks happened relatively quickly to above the $^{40}Ar/^{39}Ar$ blocking temperatures of hornblende by 39 Ma and biotite by 34 Ma. By Oligocene time some of the Lolotoi Complex had reached the surface and is unconformably overlain by basal conglomerates and limestone of the Cablac Formation. Normal faults, which assisted in the exhumation, juxtapose various Late Cretaceous to Eocene cover units with Eocene metamorphic rocks of the Lolotoi Complex. This tectonic scenario is consistent with apatite fission track model ages that indicate cooling below 120 °C during the Oligocene, then renewed burial into the partial annealing zone until rapid Pliocene–Pleistocene uplift.

Late Miocene to Pliocene opening of the Banda Sea further fragmented the Great Indonesian Arc and transported the Lolotoi Complex and its cover units (Banda Terrane) southward and eastward until they were captured in the forearc of the Banda Arc. At around 3 Ma the NW continental margin of Australia clogged the subduction channel beneath the Banda Terrane, resulting in the Late Miocene to present arc-continent collision. Collision initiated a period of rapid uplift of the Lolotoi Complex as indicated by the lack of any new fission-tracks, exposures of Late Pliocene deep marine limestone, and uplifted flights of Quaternary and Holocene coral terraces.

Structural analyses and observations of contact relationships show that during tectonic emplacement, the Lolotoi Complex was thrust over Gondwana Sequence units of the Australian continental margin as indicated by extensive outcrops of mélange and broken formation at the structural base of the Banda Terrane. This phase of deformation is recorded in the Banda Terrane by parallelism between the orientations and transport directions of structurally underlying Gondwana Sequence and the latest phases of deformation of the Banda Terrane. Duplex stacking of Gondwana Sequence units uplifted the Banda Terrane from a forearc basement position to higher than 2500 m elevation in places. Erosion has removed much of the likely continuous metamorphic terrane leaving only isolated klippen. Asian affinity overlying sedimentary and volcanic cover units are extremely attenuated by extension, yet some Oligocene units lie unconformably on portions of the Lolotoi Complex.

This study has strengthened correlations between the Mutis Complex of West Timor and Lolotoi Complex of Timor Leste, indicating that they are both part of the same Banda Terrane thrust sheet. The structural base of the Banda Terrane is the initial collisional suture between Asian and Australian affinity units. The study also provides insights into the multiply deformed nature of forearc regions, and cautions the use of metamorphic ages of a forearc nappe for the timing of collision. As the collision progresses the Banda Terrane will likely collide again with other parts of the Great Indonesian arc that have different post-metamorphic histories, which will increase the complexity of reconstructing the relatively brief events associated with arc-continent collision.

Acknowledgements

This study was funded in part by National Science Foundation grant EAR 0337221. The project would not have been possible without the assistance of the Oil, Gas and Energy Directorate (OGED) of Timor Leste (Mr. Amandio Gusmao Soares, Francisco Ferreira and Mr. Vicente de Pinto Costa and their staff), and the Natural Resources Division of Timor Leste (Lourenço Pedro and Francesco Monteira). Inacio Freitas Mereira, the Dean of the Faculty of Engineering at the National University of Timor Leste, arranged for Timorese student counterparts. We particularly wish to thank Hugo Ximenes for his assistance in the field. Eujay McCartain (Western Australia University) also helped us. We wish to thank Jeff Vervoort and Garret Hart (Washington State University) for their assistance with Hf/Lu and U/Pb age analyses. Mike Dorais and Bart Kowallis (Brigham Young University) guided our micro-probe and fission-track analyses. Richard Allmendinger gave permission to use Stereo 6. Helpful reviews were provided by Bill Dinklage, Thomas Hoisch, Michael Audley-Charles, and Ron Berry.

Appendix A. Supplementary data

Supplementary data associated with this article can be found, in the online version, at doi:10.1016/j.tecto.2009.01.034.

References

Audley-Charles, M.G., 1968. The geology of Portuguese Timor. Geological Society of London Memoir, vol. 4. 76 pp.

Audley-Charles, M.G., Carter, D.J., 1972. Palaeogeographical significance of some aspects of Paleogene and Early Neogene stratigraphy and tectonics of the Timor Sea region. Palaeogeography, Palaeoclimatology and Palaeoecology 11, 247–264.

Audley-Charles, M.G., 1986. Rates of Neogene and Quaternary tectonic movements in the southern Banda Arc based on micropaleontology. Geological Society of London 143, 161–175.

Audley-Charles, M.G., Harris, R.A., 1990. Allochthonous terranes of the Southwest Pacific and Indonesia. Philosophical Transactions of the Royal Society of London 331, 571–587.

Bailey, Willis, 1940. Philippine archipelago; an illustration of continental growth. Proceedings of the Pacific Science Congress, vol. 1, pp. 185–200.

Banno, S., Sakai, C., Higashino, T., 1986. Pressure-temperature trajectory of the Sanbagawa metamorphism deduced from garnet zoning. Lithos 19, 51–63.

Barber, A.J., Audley-Charles, M.G., 1976. The significance of the metamorphic rocks of Timor in the development of the Banda Arc, eastern Indonesia. Tectonophysics 30, 119–128.

Berry, R.F., McDougall, I., 1986. Interpretation of (super 40) Ar/ (super 39) Ar and K/Ar dating evidence from the Aileu Formation, Timor Leste, Indonesia. Chemical geology. Isotope Geoscience Section 59 (1), 43–58.

Bhatia, M.R., 1983. Plate tectonics and geochemical composition of sandstones. Journal of Geology 91, 611–627.

Bhatia, M.R., Crook, K.A.W., 1986. Trace element characteristics of greywackes and tectonic setting discrimination of sedimentary basins. Contributions to Mineralogy and Petrology 92 (2), 181–193.

Blichert-Toft, J., Frei, R., 2001. Complex Sm-Nd and Lu-Hf isotope systematics in metamorphic garnets from the Isua supracrustal belt, West Greenland. Geochimica et Cosmochimica Acta 65, 3177–3189.

Brown, M., Earle, M.M., 1983. Cordierite-bearing schists and gneisses from Timor, eastern Indonesia. *P–T* implications of metamorphism and tectonic implications. Journal of Metamorphic Geology 1, 183–203.

Carter, D.J., Audley-Charles, M.G., Barber, A.J., 1976. Stratigraphical analysis of island arc-continental margin collision in eastern Indonesia. Geological Society of London 132, 179–198.

Chamalaun, F.H., Grady, A.E., 1978. The tectonic evolution of Timor. A new model and its implications for petroleum exploration. Journal of the Australian Petroleum Exploration Association 18, 102–108.

Charlton, T.R., 2002. The structural setting and tectonic significance of the Lolotoi, Laclubar and Aileu metamorphic massifs, Timor Leste. Journal of Asian Earth Sciences 20, 851–865.

Cox, N.L., Harris, R.A., Merritts, D., 2006. Quaternary uplift of coral terraces from active folding and thrusting along the northern coast of Timor–Leste. Eos Trans. AGU 87 (52), T51D–1564.

de Roever, W.P., 1940, Geological Investigation in the Southwestern Moetis Region (Netherlands Timor) [Ph.D. Thesis]: University of Amsterdam, 244 pp.

de Waard, D., 1954a. Contributions to the geology of Timor 2; the orogenic main phase in Timor. Indonesian Journal of Natural Science 110, 9–20.

de Waard, D., 1954b. Contributions to the Geology of Timor 5. Structural developments of the crystalline schists in Timor, tectonics of the Lalan Asu massif. Indonesian Journal for Natural Science 110, 143–153.

de Waard, D., 1957. Zones of regional metamorphism in the Lalan Asu massif, Timor. K. Nederl. Akad. Wetens., vol. 60, pp. 383–392. no. 5.

de Waard, D., 1959. Anorthite content of plagioclase in basic and pelitic crystalline schists as related to metamorphic zoning in the Usu massif, Timor. American Journal of Science 257, 553–562.

Donelick, R.A., O'Sullivan, P.B., Ketcham, R.A., 2005. Apatite fission-track analysis. In: Reiners, P.W., Ehlers, T.A. (Eds.), Low-Temperature Thermochronology. Techniques, Interpretations, and Applications. Virginia, The Mineralogical Society of America, vol. 58, pp. 48–94.

Earle, M.M., 1980, A Study of Boi and Mollo, Two Metamorphic Massifs on Timor, Eastern Indonesia. [Ph.D Thesis]: University of London, 240 pp.

Earle, M.M., 1981. The metamorphic rocks of Boi, Timor, eastern Indonesia. In: Barber, A.J., Wiryosujono, S. (Eds.), The Geology and Tectonics of Eastern Indonesia. GRDC Special Publication, vol. 2, pp. 239–251.

Fallon, T.J., Berry, R.F., Robinson, P., Stolz, A.J., 2006. Whole-rock geochemistry of the Hili Manu peridotite, East Timor. Implications for the origin of Timor ophiolites. Australian Journal of Earth Sciences 53, 637–649.

Fleischer, R.L., Price, P.B., Walker, R.M., 1964. Fission-track ages of zircons. Journal of Geophysical Research 69, 4885–4888.

Floyd, P.A., Winchester, J.A., 1975. Magma type and tectonic setting discrimination using immobile elements. Earth and Planetary Science Letters 27, 211–218.

Gageonnet, R., Lemoine, M., 1958. Contribution a la connaissance de la geologie de la province Porugaise de Timor. Monograph, Portugal, Ministerio Ultramar, Est. 48.

Gerya, T.V., Perchuk, L.L., Audren, C., Sez'ko, A.I., 1997. Petrology of the Tumanshet zonal metamorphic complex, eastern Sayan. Petrology 5, 503–533.

Grady, A.E., 1975. A reinvestigation of thrusting in Portuguese Timor. Journal of the Geological society of Australia 22, 223–227.

Grady, A.E., Berry, R.F., 1977. Some Paleozoic–Mesozoic stratigraphic-structural relationships in Timor Leste and their significance to the tectonics of Timor. Journal of the Geological Society of Australia 24, 203–214.

Haig, D.W., McCartain, E., Barber, L., Backhouse, J., 2007. Triassic–Lower Jurassic foraminiferal indices for Bahaman-type carbonate-bank limestones, Cablac Mountain, East Timor. Journal of Foraminiferal Res. 37, 248–264.

Haile, H.S., Barber, A.J., Carter, D.J., 1979. Mesozoic cherts on crystalline schists in Sulawesi and Timor. Geological Society of London 136, 65–70.

Hamilton, W., 1979. Tectonics of the Indonesian region. U.S. Geological Survey Professional Paper 1078 345 pp.

Harris, R.A., 1991. Temporal distribution of strain in the active Banda Orogen. A reconciliation of rival hypotheses. Journal of Southeast Asian Earth Sciences 6, 373–386.

Harris, R.A., 1992. Peri-collisional extension and the formation of Oman-type ophiolites in the Banda Arc and Brooks Range. In: Parson, L.M., Murton, B.J., Browning (Eds.), Ophiolites and their Modern Oceanic Analogues. Geological Society of London Special, Publication, vol. 60, pp. 301–325.

Harris, R., 2006. Rise and fall of the Eastern Great Indonesian arc recorded by the assembly, dispersion and accretion of the Banda Terrane, Timor. Gondwana Research 10, 207–231.

Harris, R.A., Long, T., 2000. The Timor ophiolite, Indonesia. Model or myth? In: Dilek, Y., Moores, E.M., Elthon, D., Nicolas, A. (Eds.), Ophiolites and Oceanic Crust. New Insights from Field Studies and the Ocean Drilling Program. Geologic Society of America Special Paper, vol. 349, pp. 321–330.

Harris, R.A., Sawyer, R.K., Audley-Charles, M.G., 1998. Collisional mélange development. Geologic associations of active mélange-forming processes with exhumed mélange facies in the western Banda Orogen, Indonesia, vol. 17, pp. 458–479.

Harris, R.A., Kaiser, J., Hurford, A., Carter, A., 2000. Thermal history of Australian passive margin cover sequences accreted to Timor during Late Neogene arc-continent collision, Indonesia. Journal of Asian Earth Science 18, 47–69.

Harris, R.A., Vorkink, M.W., Prasetyadi, C., 2009. Transition from subduction to arc-continent collision. geological and neotectonic evolution of Sawu, Indonesia. Geosphere 5, 152–171.

Honthaas, C., Rehault, J., Maury, R., Bellon, H., Hemond, C., Malod, J.A., Cornee, J.J., Villeneuve, M., Cotten, J., Burhanuddin, S., Guillou, H., Arnaud, N., 1998. A Neogene back-arc origin for the Banda Sea basins: geochemical and geochronological constraints from the Banda ridges (East Indonesia). Tectonophysics 298, 297–317.

Jahn, Bor-ming, Griffin, W.L., Windley, B.F., 1998. Continental growth in the Phanerozoic; evidence from Central Asia. Tectonophysics 328, 1–227.

Kaneko, Y., Maruyama, S., Kadarusman, A., Ota, T., Ishikawa, M., Tsujimori, T., Ishikawa, A., Okamoto, K., 2007. On-going orogeny in the outer-arc of the Timor–Tanimbar region, eastern Indonesia. Gondwana Research 11, 218–233.

Ketcham, R.A., Donelick, R.A., Donelick, M.B., 2003. AFTSolve; a program for multi-kinetic modeling of apatite fission-track data. American Mineralogist 88, 929.

Kleemann, U., Reinhardt, J., 1994. Garnet–biotite thermometry revisited; the effect of Al (super VI) and Ti in biotite. European Journal of Mineralogy 6, 925–941.

Kohn, M.J., Spear, F., 2000. Retrograde net transfer reaction insurance for pressure–temperature estimates. Geology 28, 1127–1130.

Leake, B.E., 1997. Nomenclature of amphiboles. Report of the subcommittee on amphiboles of the International Mineralogical Association, commission on new minerals and mineral names. American Mineralogist 82, 1019–1037.
Lunt, P., 2003. Biogeography of some Eocene larger foraminifera, and their application in distinguishing geological plates. Palaeontologia Electronica 6, 1–22.
Lytwyn, J., Rutherford, E., Burke, K., Xia, C., 2001. The geochemistry of volcanic, plutonic, and turbiditic rocks from Sumba, Indonesia. Journal of Asian Earth Sciences 19, 481–500.
McDonough, W.F., Sun, S.-s., 1995. The composition of the Earth. Chemical Geology 120, 223–253.
Mezger, K., 1990. Geochronology in granulites. In: Vielzeuf, D., Vidal, P. (Eds.), Granulites and crustal evolution: NATO ASI Series C:. Mathematical and Physical Sciences, vol. 311, pp. 451–470.
Milsom, J., Sardjono, R., Susilo, A., 2001. Short-wavelength, high-amplitude gravity anomalies around the Banda Sea, and the collapse of the Sulawesi orogen. Tectonophysics 333, 61–74.
Naeser, C.W., 1976. Fission-track dating. U.S. Geological Survey Open-File Report, 76–190. 65 pp.
Naeser, C.W., 1979. Fission-track dating and geologic annealing of fission-tracks. In: Jager, E., Hunziker, J.C. (Eds.), Lectures in Isotope Geology. Springer Verlag, New York, pp. 154–169.
Naeser, C.W., Dodge, F.C.W., 1969. Fission-track ages of accessory minerals from granitic rocks of the Central Sierra Nevada Batholith, California. Bulletin of the Geological Society of America 80, 2201–2212.
Naeser, N.D., Naeser, C.W., McCulloh, T.H., 1989. The application of fission-track dating to the depositional and thermal history of rocks in sedimentary basins. In: Naeser, N.D., McCulloh, T.H. (Eds.), Thermal History of Sedimentary Basins. Springer-Verlag, New York, pp. 157–180.
Newton, R.C., Haselton, H.T., 1981. Thermodynamics of the garnet–plagioclase–Al (sub 2) SiO (sub 5) –quartz geobarometer. In: Saxena, S.K. (Ed.), Thermodynamics of minerals and melts. Springer-Verlag, New York, pp. 131–147.
Patchett, P.J., Tatsumoto, M., 1980. A routine high precision method for Lu–Hf isotope geochemistry and chronology. Contributions to Mineral Petrology 75, 263–267.
Patchett, P.J., Ruiz, J., 1987. Nd isotopic ages of crust formation and metamorphism in the Precambrian of eastern and southern Mexico. Contributions to Mineral Petrology 75, 523–528.
Pearce, J.A., 1982. Trace element characteristics of lavas from destructive plate boundaries. In: Thorpe, R.S. (Ed.), Andesites. Wiley, Chicchester, pp. 525–548.
Pearce, J.A., 1996. A users guide to basalt discrimination diagrams. In: Wyman, D.A. (Ed.), Trace Element Geochemistry of Volcanic Rocks: Applications for Massive Sulfide Exploration. Geological Association of Canada, Short Course Notes, vol. 12, pp. 79–113.
Pearce, J.A., Cann, J.R., 1973. Tectonic setting of basic volcanic rocks determined using trace element analyses. Earth and Planetary Science Letters 19, 290–300.
Pearce, J.A., Gale, G.H., 1977. Identification of ore-deposition environment from trace-element geochemistry of associated igneous host rocks:. Joint meeting of the Geological Society of London, Volcanic Studies Group, Institution of Mining and Metallurgy, London.
Prasetyadi, C., Harris, R.A., 1996. Hinterland structure of the active Banda arc-continent collision, Indonesia: constraints from the Aileu Complex of Timor Leste. Proc. 25th Conv. Indonesian Association of Geology, pp. 144–173.
Rollinson, H., 1993. Using geochemical data: evaluation, presentation, interpretation. Longman Sigamore Publishers, England. 352 pp.
Roser, B.P., Korsch, R.J., 1988. Provenance signatures of sandstone–mudstone suites determined using discriminant function analysis of major-element data. Chemical Geology 67, 119–139.
Roosmawati, N., Harris, R.A., 2009. Surface uplift history of the incipient Banda arc-continent collision: Geology and synorogenic foraminifera of Rote and Savu Islands, Indonesia. Tectonophysics 479, 95–110 (this issue).
Searle, M.P., Stevens, R.K., 1984. Obduction processes in ancient, modern and future ophiolites. In: Gass, I.G., Lippard, S.J., Shelton, A.W. (Eds.), Ophiolites and oceanic lithosphere. Geol. Soc. of London Spec. Pub., vol. 13, pp. 303–320.
Smyth, H.R., Hamilton, P.J., Hall, R., Kinny, P.D., 2007. The deep crust beneath island arcs: inherited zircons reveal a Gondwana continental fragment beneath East Java, Indonesia. Earth and Planetary Science Letters 258, 269–282.
Sopaheluwaken, J., 1990, Ophiolite obduction in Mutis Complex, Timor, Eastern Indonesia: An Example of Inverted, Isobaric, Medium-High Pressure Metamorphism. [PhD Thesis]: Amsterdam, Free University.
Sopaheluwaken, J., Helmers, H., Tjokrosapoetro, S., Surya, N.E., 1989. Medium pressure metamorphism with inverted thermal gradient associated with ophiolite emplacement in Timor. Neatherlands Journal of Sea Research 24, 333–343.
T'Hoen, C.W.A.P., van Es, L.J.C., 1926. The exploration for minerals in the island of Timor. Jaarb. Mijn. Ned. Indie, vol. 2, pp. 1–80.
Tappenbeck, D., 1939, Geologiedes Mollogebirges und Einiger Benachbanen Gebiete (Niederlandisch Timor). [Ph.D. Thesis]: Amsterdam.
Taylor, S.R., McClennan, S.M., 1985. The continental crust. Its Composition and Evolution; an Examination of the Geochemical Record Preserved in Sedimentary Rocks. Blackwell Sci. Publ., Oxford, United Kingdom. 312 pp.
van Leeuwen, T.M., 1981. The geology of Southwest Sulawesi with special reference to the Biru area. Geol. Res. Centre. Indonesia Spec. Publ., vol. 2, pp. 277–304.
van West, F.P., 1941, Geological investigations in the Miomaffo region [Ph.D. Thesis]: Amsterdam.
Vervoort, J.D., Patchett, P.J., 1996. Behavior of halfnium and neodymium isotopes in the crust: constraints from Precambrian crustally derived granites. Geochimica et Cosmochimica Acta 60, 3717–3733.
Vervoort, J.D., Blichert-Toft, J., 1999. Evolution of the depleted mantle: Hf isotope evidence from juvenile rocks through time. Geochimica et Cosmochimica Acta 63, 533–556.
Vervoort, J.D., Patchett, J.P., Soderlund, U., 2004. Isotopic composition of Yb and the determination of Lu concentrations and Lu/Hf rations by isotope dilution using MC-ICPMS. Geochemistry, Geophysics, Geosystems 5, 1–15.
Wanner, J., 1913. Geologie von West Timor. Geologische Rundschau 4, 136–150.
Winchester, J.A., Floyd, P.A., 1976. Geochemical magma type discrimination; application to altered and metamorphosed basic igneous rocks:. Earth and Planetary Science Letters 28, 459–469.
Zobell, E.A., Harris, R.A., 2007. New insights into the stratigraphic and structural evolution of the active Banda Orogen, Abst. Geological Society of America 39, 45.